

<https://doi.org/10.18321/1099>

*This paper is devoted to the celebration  
of 75 years' jubilee of Professor Zulkhair Mansurov*

## Promoters for Improvement of the Catalyst Performance in Methane Valorization Processes

I.Z. Ismagilov<sup>1</sup>, A.V. Vosmerikov<sup>2</sup>, L.L. Korobitsyna<sup>2</sup>, E.V. Matus<sup>1</sup>,  
M.A. Kerzhentsev<sup>1</sup>, A.A. Stepanov<sup>2</sup>, E.S. Mihaylova<sup>3</sup>, Z.R. Ismagilov<sup>1,3\*</sup>

<sup>1</sup>Boreskov Institute of Catalysis, Siberian Branch, Russian Academy of Sciences,  
pr. Akademika Lavrentieva, 5, Novosibirsk, Russia

<sup>2</sup>Institute of Petroleum Chemistry, Siberian Branch, Russian Academy of Sciences,  
pr. Akademicheskiy, 4, Tomsk, Russia

<sup>3</sup>Federal Research Center of Coal and Coal Chemistry, Siberian Branch of the Russian Academy of Sciences,  
pr. Sovetskiy, 18, Kemerovo, Russia

### Article info

Received:  
12 February 2021

Received in revised form:  
17 April 2021

Accepted:  
5 June 2021

### Keywords:

Catalyst  
Promoters  
Nanoparticles  
Methane  
Dehydroaromatization  
Autothermal reforming

### Abstract

In this work, the introduction of modifying additives in the composition of catalysts is considered as an effective mode of improving functional characteristics of materials for two processes of methane conversion into valuable products – methane dehydroaromatization (DHA of CH<sub>4</sub>) into benzene and hydrogen and autothermal reforming of methane (ATR of CH<sub>4</sub>) into synthesis gas. The effect of type and content of promoters on the structural and electronic state of the active component as well as catalyst activity and stability against deactivation is discussed. For DHA of CH<sub>4</sub> the operation mode of additives M = Ag, Ni, Fe in the composition of Mo-M/ZSM-5 catalysts was elucidated and correlated with the product yield and coke content. It was shown that when Ag serves as a promoter, the duration of the catalyst stable operation is enhanced due to a decrease in the rate of the coke formation. In the case of Ni and Fe additives, the Ni-Mo and Fe-Mo alloys are formed that retain the catalytic activity for a long time in spite of the carbon accumulation. For ATR of CH<sub>4</sub>, the influence of M = Pd, Pt, Re, Mo, Sn in the composition of Ni-M catalysts supported on La<sub>2</sub>O<sub>3</sub> or Ce<sub>0.5</sub>Zr<sub>0.5</sub>O<sub>2</sub>/Al<sub>2</sub>O<sub>3</sub> was elucidated. It was demonstrated that for Ni-M/La<sub>2</sub>O<sub>3</sub> catalysts, Pd is a more efficient promoter that improves the reducibility of Ni cations and increases the content of active Ni<sup>0</sup> centers. In the case of Ni-M/Ce<sub>0.5</sub>Zr<sub>0.5</sub>O<sub>2</sub>/Al<sub>2</sub>O<sub>3</sub> samples, Re is considered the best promoter due to the formation of an alloy with anti-coking and anti-sintering properties. The use of catalysts with optimal promoter type and its content provides high efficiency of methane valorization processes.

## 1. Introduction

Catalytic processes play a crucial role in our lives. Biocatalysts – enzymes – control all biochemical processes in nature and, in essence, underlie life on Earth [1, 2]. In the industry, catalysts are employed in more than 90% of current chemical processes and involved in the processing of over 20% of all manufactured products [3]. Except

for the synthesis of bulk chemicals, the catalytic reactions serve as a basis for oil refining and petrochemistry, processing of polymers, pharmaceuticals, and purification of exhaust gases. The application of catalysts makes chemical processes more efficient, increases the product quality and operating profit as well as contributes to environmental protection. So, the catalytic process is a key factor for the sustainable development of industrial society [4–7]. The world catalyst market is estimated at \$35.5 billion [8]. Growth of the market is expected

\*Corresponding author. E-mail: [zinfer1@mail.ru](mailto:zinfer1@mail.ru)

due to a rise in expenses for the production of the derivatives of petroleum through syngas.

Compared with traditional areas of catalyst application, the gas chemical sector is not so significant. Natural gas (NG) and associated petroleum gas (APG), as well as new types of gas raw materials – coal mine methane and biogas, are valuable raw materials for the production of various chemical products. For example, oil production is accompanied by the release of APG – up to several thousand cubic meters per 1 t of oil. Its main components are methane (67–92%) and ethane (2–14%). However, currently in Russia, the use of NG and APG as raw materials for the chemical industry is limited to 10% [9]. The major part of these gases is used as a fuel for the generation of electrical and heat energy or simply destroyed by burning in flame both at large deposits and at numerous small deposits located in areas far away from transport and pipelines or in hard-to-reach regions. This results in an irretrievable loss of valuable hydrocarbon raw materials. Also, the concomitant emission of a huge amount of  $\text{CO}_x$ , dust, soot and toxic substances leads to environmental pollution and is the cause of serious environmental problems. So, considerable resources and availability of these raw materials, as well as the need to move to resource-saving processes, create favorable conditions for the development of improved catalytic technologies for methane valorization.

The catalytic process of methane valorization can be divided into direct and indirect ways (Fig. 1).

The catalytic decomposition of methane into carbon and hydrogen [10, 11], methane dehydroaromatization to benzene [12–23], methane oxidation to methanol [24, 25] and formaldehyde [25, 26], oxidative coupling of methane [27–35] are the most thoroughly studied methods of the direct

methane conversion. One of the promising directions of natural gas (methane) processing is its direct transformation into a mixture of liquid hydrocarbons  $\text{C}_6\text{--C}_{12}$  on zeolite-containing catalysts. The recognized most efficient catalysts for this process are Mo-containing systems based on high-silica zeolite of the ZSM-5 type. However, to date, one-stage processes of methane conversion do not have economic advantages over indirect ways of methane processing.

The main product of the indirect methane processing is commonly the synthesis gas that can be produced via methane steam reforming ( $\text{CH}_4 + \text{H}_2\text{O} = \text{CO} + 3\text{H}_2$ ), methane carbon dioxide reforming ( $\text{CH}_4 + \text{CO}_2 = 2\text{CO} + 2\text{H}_2$ ) or through methane partial oxidation ( $\text{CH}_4 + 1/2\text{O}_2 = \text{CO} + 2\text{H}_2$ ) [36]. The main process for syngas production is the steam reforming of methane. The catalyst activity depends primarily on the composition of the active component, and it increases in the following sequence of metals [37]: Rh, Ru>>Ni>Ir>Pd, Pt, Co, Fe. Due to the high price of noble metals commercial steam reforming catalysts are based on nickel deposited on various supports ( $\text{Al}_2\text{O}_3$ ,  $\text{MgO}$ ,  $\text{MgAl}_{12}\text{O}_4$ ,  $\text{ZrO}_2$ ). The reaction proceeds at 900–1000 °C, pressure 1.5–3 MPa, and gas hourly space velocities ~1000 h<sup>-1</sup> [38–41]. The methane conversion with  $\text{CO}_2$  is conducted at temperatures above 700 °C [36]. The most efficient catalysts for this reaction are platinum group metals [42] and metals of the iron group [43] on various supports. The partial oxidation of methane is also carried out at high temperatures over 750 °C and systems based on noble metals and nickel serve as catalysts for this process [44]. The methane steam reforming is an endothermic reaction, therefore it requires the supply of heat. The autothermal methane reforming that additionally includes exothermal reactions of

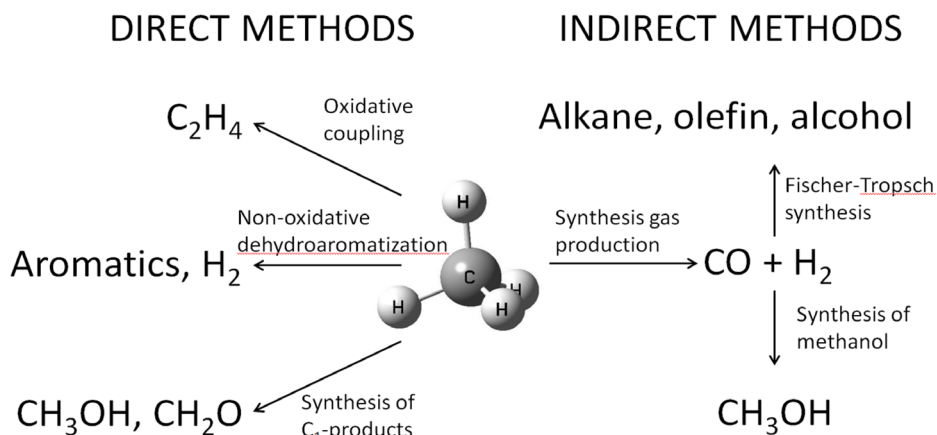


Fig. 1. Main processes of methane valorization.

methane oxidation provides a more advantageous energy balance. The energy effect of this process can be controlled by the variation of the ratio of reagents – methane, oxygen, and water:



$$\Delta H^\circ_{298\text{K}} = 206.2 - 241.8 \cdot x \text{ kJ/mol}$$

In addition to the advantageous energy balance, this reaction leads to higher hydrogen yield and is characterized by increased resistance to the formation of carbon deposits owing to the presence of oxygen in the reaction mixture. The most widely used catalysts for the methane conversion into hydrogen-containing gas are nickel-based ones on various oxide supports [45–52]. The produced synthesis gas is used in the catalytic synthesis of methanol, production of synthetic gasoline, diesel fuel and dimethyl ether [38, 53, 54]. In all cases, final commercial products are obtained through several intermediate stages, which increases the product price, while the capital investments in the installation for the syngas production can attain 70% of all expenses required for the production of the target product.

With a call for green chemistry, environmental regulations, rising raw material prices, and heavier feedstock the up-grading of existing catalysts or the creation of new catalytic systems are required. It is a grand challenge to develop a catalytic material that would be characterized by high activity and stability as well as providing near-100% selectivity to the desired product with minimal use of energy [4]. There are different approaches to the improvement of catalyst performance and reduction of the deactivation rate. The specifics of the strategy will depend on the chemical composition and physicochemical properties of the catalyst and the mechanism of its deactivation in real conditions of the catalytic process. It is known [55–64] that the introduction of modifying additives into the catalyst composition allows the control of the dispersion and redox properties of the active component and correspondingly the improvement of the activity and stability of catalytic systems. For the development of methods for direct regulation of catalyst physicochemical properties and activity it is interesting to carry out a comparative study of the effects of different additives on the catalyst physicochemical properties and functional characteristics in methane conversion to value-added chemical products and semi-products. The present

work gives a brief analysis of the literature data and the positive experience of the authors in the development of promoted catalysts for the dehydroaromatization of methane to benzene and hydrogen and methane autothermal reforming to syngas. On the basis of comparing results of characterization of catalysts by a complex of instrumental methods (low-temperature nitrogen adsorption, X-ray diffraction, transmission electron microscopy, temperature-programmed reduction by hydrogen) and their catalytic activity, the interrelation “composition-structure-properties” has been established, and the optimal additives (both type and content) for each process have been found.

## 2. Dehydroaromatization of methane

The most efficient systems for methane dehydroaromatization are Mo/ZSM-5 catalysts. The usual widely employed method for the synthesis of Mo-containing zeolite catalysts is the method of zeolite impregnation with a solution of ammonium paramolybdate  $(\text{NH}_4)_6\text{Mo}_7\text{O}_{24} \cdot 4\text{H}_2\text{O}$  [65–67]. The concentration of the impregnating solutions is varied in a wide range. The Mo content in the dried catalyst samples is within a range of 1–20 wt.% [68–72]. The conditions for the preparation of Mo-ZSM-5 catalysts (conditions of impregnation, duration and temperature of thermal treatment, pretreatment with different gases, etc.) are also diverse, which makes difficult the comparison of the results obtained by different authors. In addition to the impregnation method, for the preparation of Mo-ZSM-5 catalysts, a method of solid-phase synthesis is used. In this case, zeolite is mixed with salt or an oxide of molybdenum, the mixture is dried and then calcined at 500 °C [73, 74].

The study of the activity of catalysts obtained by the solid-phase synthesis showed that these catalysts could be both more [75] and less active [73] than the ones prepared by the impregnation method. The main reason for the difference in the activity of catalysts prepared by different methods, according to the opinion of many authors, is the different localization of molybdenum in catalysts. For example, the XPS study of Mo/ZSM-5 samples prepared by the impregnation method shows that in these catalysts more strong interaction of Mo with the zeolite matrix takes place as compared to samples obtained by the solid-state synthesis. This interaction hinders the formation of molybdenum carbide particles necessary for the reaction, thus resulting in the lower activity of the impregnated catalysts.

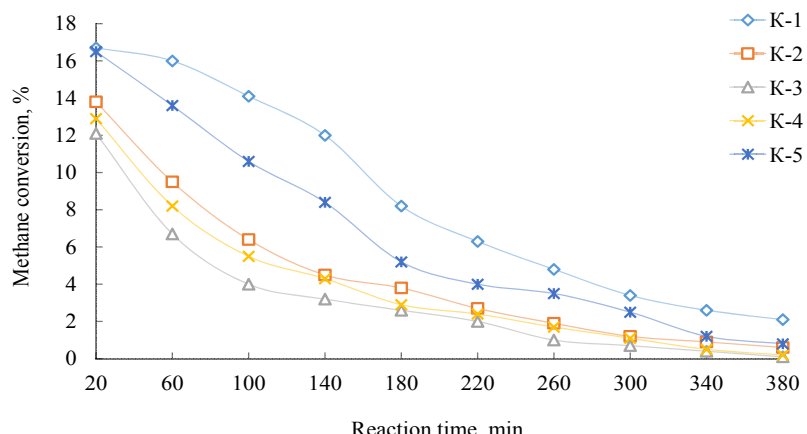


Fig. 2. Dependence of methane conversion on the reaction time on catalysts prepared with the use of different molybdenum compounds (4.0 wt. %): K-1 – Mo(NSP)/ZSM-5; K-2 – MoO<sub>3</sub>(NSP)/ZSM-5; K-3 – Mo<sub>2</sub>C(NSP)/ZSM-5; K-4 – MoO<sub>3</sub> (techn.)/ZSM-5; K-5 – Mo/ZSM-5 (impregnation) [76].

The work [76] describes the results of the study of the catalytic activity and stability of Mo/ZSM-5 catalysts prepared by the solid-phase synthesis with the use of nanosized powders (NSP) of Mo and its compounds (Mo<sub>2</sub>C and MoO<sub>3</sub>). In addition, a comparative analysis of the properties of the obtained catalysts with those prepared by the traditional impregnation method and a method employing the use of technical grade molybdenum anhydride was carried out. The authors of [65] showed that the activity and stability of Mo-containing zeolite catalyst depend primarily on the type of molybdenum compound used for its preparation. It is connected mainly with molybdenum distribution over the surface and in the zeolite channels. Figure 2 shows the results of the study of the activity and stability of Mo/ZSM-5 catalyst prepared by different methods in the process of methane conversion. It can be seen that the sample containing Mo<sub>2</sub>C exhibits lower activity in this process despite the opinion of some researchers that carbides and oxycarbides of molybdenum should act as methane activation sites [77, 78]. Low activity of Mo/ZSM-5 catalysts prepared with the use of Mo<sub>2</sub>C is also noted in [66].

The catalyst prepared by the mechanical mixing of zeolite with Mo nanosized powder and the subsequent oxidation in air at the calcination of the mixture exhibits the highest activity. The molybdenum distribution over the surface and in the zeolite channels in this catalyst appears to be different from those in Mo-containing samples prepared with the use of preliminarily oxidized Mo NSP, molybdenum anhydride and carbide of Mo. It is known [65] that during the calcination of Mo compounds deposited onto zeolite the localization of MoO<sub>3</sub> on the outer zeolite surface occurs with

some fraction of Mo migrating into the zeolite channels. The probability of the penetration of Mo nanoparticles into the zeolite channels is higher than of MoO<sub>3</sub> and Mo<sub>2</sub>C particles due to its higher dispersion. The particles of Mo oxide localized on the zeolite surface can be easily reduced to Mo<sub>2</sub>C by methane, while Mo compounds in the zeolite channels are reduced at a lower rate and remain partly oxidized, which affects the catalyst performance in the reaction of methane dehydroaromatization [79]. Thus, it can be concluded that the nanosized powder of Mo is an efficient additive to the ZSM-5 zeolite because of its high dispersion that facilitates its migration into the zeolite bulk during the catalyst preparation and results in an increase of the catalyst activity and stability.

The products of the methane conversion on the catalyst 4.0% Mo(NSP)/ZSM-5 contain mainly ethane, ethylene, benzene, and naphthalene (Fig. 3). The total yield of ethane and ethylene increases during the process progression attaining the maximum values at 220–300 min of the reaction time, then the formation of ethane and ethylene declines due to the carbonization of the catalyst active sites. The highest amounts of benzene and naphthalene form during the first 20 min of the reaction, then their concentration decreases.

Many scientific works are devoted to the study of the molybdenum state in the zeolite matrix. However, there is no unambiguous opinion about the localization of Mo in the initial Mo/ZSM-5 catalysts prepared by different methods. This is explained by numerous factors affecting Mo state and its localization in zeolite: molybdenum content [69], temperature [69, 80], calcination duration and the composition of the gas medium during

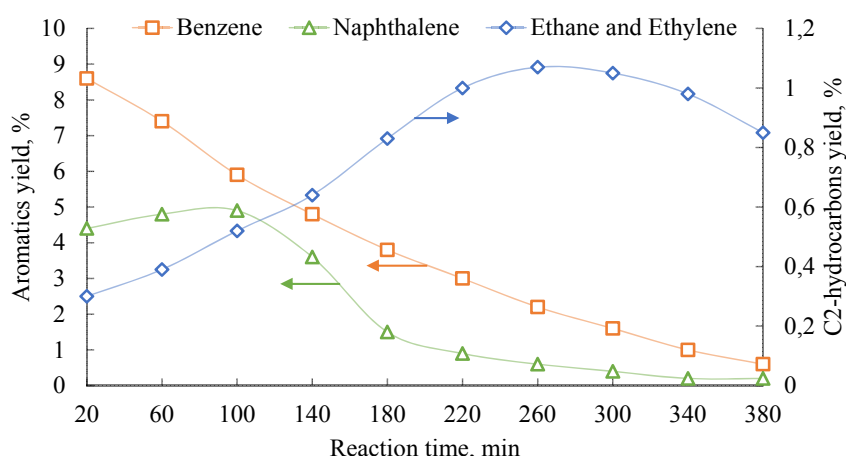


Fig. 3. The yield of the products of methane dehydroaromatization on the catalyst 4.0% Mo(NSP)/ZSM-5.

calcination [80, 81], etc. The obtained experimental results point to the presence of Mo on the outer zeolite surface and its stabilization in the zeolite channels. The generally accepted notion is the transformation of molybdenum oxide phases to carbide compounds in the course of the reaction of methane dehydroaromatization. It is noted that in the case of the solid-phase synthesis Mo is predominantly localized in the zeolite channels.

The variation of the chemical composition of Mo/ZSM-5 catalysts by the introduction of modifying additives is one of the most effective approaches to improve the process of methane dehydroaromatization. In several works [82–85] it was shown that the presence of a second metal in addition to molybdenum, can have a substantial effect on the activity, selectivity, and resistance to the coking of Mo/ZSM-5 catalysts. A wide range of metals were studied as promoters: Fe [85–87], Co [86, 88], Ni [83, 89], Cu [88, 90], Zn [87, 91, 92], Ga [93, 94], Cr [95], Ag [84, 96], Pd [97], Ir [97], V [98], Pt [99], Ru [100], La [101], P [102], etc. The data on nature (Ni, Ti, Zr, W, Ru, La, Ce, platinum group metals, etc.) and the content (from 0.01 to 10 wt.%) of the promoting additive are rather diverse.

Table 1 presents the literature data on the activity of various Me-Mo/ZSM-5 catalysts. It is shown that the introduction of the second metal into the Mo/ZSM-5 system allows improvement of the activity and selectivity of the catalyst and also a decrease in the degree of the catalyst coking. It appears that the data on the optimum content, method of the introduction and forms of the stabilization of a promoting additive are rather contradictory. Investigations showed that the additions of Ru, Zn, Cu, Zr, Fe, V, and W resulted in an increase of the selectivity as well as the stability of the operation

of Mo/ZSM-5 catalysts, while the role of Co and Pt remained controversial. In [103] it was noted that the addition of Pt to the catalyst 2% Mo/ZSM-5 did not lead to a substantial improvement of the catalyst performance, however, the methane conversion on the Pt-promoted catalyst increased a little. Another work [104] showed that the addition of Pt resulted in increased methane conversion, but the benzene yield was decreased.

The introduction of copper by ion-exchange into the initial H-ZSM-5 zeolite with the subsequent solid-phase synthesis of Mo/Cu/ZSM-5 (Cu/ZSM-5 + MoO<sub>3</sub>) allows the preparation of more active and stable catalyst [106]. The study of this catalyst after the reaction by XPS and ESR showed that the presence of copper promoted an increase in the content of Mo<sup>5+</sup> ions in the sample. Besides, XRD and NMR<sup>27</sup>Al studies revealed that the introduction of copper decreased the rate of the zeolite dealumination and its coking thus increasing the catalyst operation time. The nature of the carbon deposits also changed: the temperature of their oxidation decreased and the amount of carbonaceous radicals increased.

It was shown that the additions of Co [86], W [105], Zr [98], and Ru [100] into Mo/ZSM-5 catalyst increased its activity and selectivity. The improved performance of Mo/ZSM-5 catalysts modified by Ru is connected with a decrease of the number of strong and an increase in the number of weak and medium Broensted acid centers (BAC), and also with the more facile reduction of the initially formed molybdenum oxide. The use of Pt as a modifying additive leads to an increase in the stability of Mo/ZSM-5 catalyst resulting from a decrease in the amount of carbonaceous deposits formed during the reaction [103].

**Table 1**  
The influence of the nature of a promoting additive on the activity of Mo/ZSM-5 catalysts  
for methane dehydroaromatization [105]

Catalyst	Reaction conditions	Methane conversion, %	Selectivity, %	
			Aliphatic HC	Aromatic HC
0.5%Pt-2%Mo/ZSM-5	1400 ml/(g·h) 700 °C	5.9	4.7	79.1
1.0%Pt-2%Mo/ZSM-5	1400 ml/(g·h) 700 °C	6.4	4.6	82.2
1.0%La-2%Mo/ZSM-5	1440 ml/(g·h) 650 °C	3.3	6.1	93.9
0.5%W-2%Mo/ZSM-5	1440 ml/(g·h) 650 °C	4.0	5.0	95.0
1.0%V-2%Mo/ZSM-5	1440 ml/(g·h) 650 °C	2.7	11.1	88.9
1.0%Zr-2%Mo/ZSM-5	1440 ml/(g·h) 650 °C	5.2	5.8	94.2
0.1%Li-2%Mo/ZSM-5	1400 ml/(g·h) 700 °C	4.2	23.1	65.7
0.5%Li-2%Mo/ZSM-5	1400 ml/(g·h) 700 °C	1.3	56.8	31.3
0.1%P-2%Mo/ZSM-5	1400 ml/(g·h) 700 °C	5.4	8.7	79.8
0.5%P-2%Mo/ZSM-5	1400 ml/(g·h) 700 °C	4.6	8.4	75.7
1.2%Rh-6%Mo/ZSM-5	2700 ml/(g·h) 750 °C	7.1	6.9	93.1
1.2%Pt-6%Mo/ZSM-5	2700 ml/(g·h) 750 °C	7.2	6.7	93.3
0.3%Pt-2%Mo/ZSM-5	1600 ml/(g·h) 700 °C	5.4	4.2	89.5
0.3%Pd-2%Mo/ZSM-5	1600 ml/(g·h) 700 °C	5.2	3.1	91.1
0.3%Ru-2%Mo/ZSM-5	1600 ml/(g·h) 700 °C	4.9	4.0	89.7
0.3%Ir-2%Mo/ZSM-5	1600 ml/(g·h) 700 °C	4.6	4.4	88.3

At the introduction of Fe (Fe/Mo(mol.) = 0.25) an increase in the activity and stability of the catalyst operation takes place [86]. However, as it follows from the data of the elemental analysis, the amount of carbonaceous deposits increases simultaneously. Taking into account that the duration of the experiment did not exceed 6 h the observed improvement of the catalyst performance could not be expected to last long. Concerning the Co additive, no positive effect of its introduction was observed in this work.

The presence of vanadium in Mo/ZSM-5 catalyst decreases its activity [98] which is due to a decrease in the number of BAC participating in the reaction of methane dehydroaromatization.

In [83–85] the results of the study of catalytic activity and stability of Mo/ZSM-5 catalysts promoted by nanosized powders (NSP) of Ag, Ni, and Fe are described. All samples were prepared by the method of solid-phase synthesis in a ball vibratory mill. The content of Mo in the zeolite was 4 wt.%, and the contents of the modifying additives were varied in a range from 0.05 to 2.0 wt.%. The highest activity and stability were exhibited by the catalysts M-4.0% Mo/ZSM-5 containing 0.1 wt.% of the studied metals. The increase of the content of a modifying additive over 1.0 wt.% leads to a

substantial decrease in the activity and stability of M-4.0% Mo/ZSM-5 catalysts.

Using methods of high-resolution transmission electron microscopy and spectroscopy of X-ray characteristic radiation it was shown that the microstructure and composition of the prepared catalytic systems and the nature of the formed surface coke are different. For instance, in the initial Ni-4.0% Mo/ZSM-5 samples after calcination at 550 °C oxide particles MoO<sub>3</sub> and NiO with a size of 10–50 nm (Fig. 4) are formed with a part of these particles being in a coarsely dispersed state (sizes ca. 50 nm) [83].

In the samples after the reaction, Ni and Mo particles fundamentally different by their morphology, composition, and character of their localization in the zeolite ZSM-5 were observed. On the surface of the zeolite crystals, there are particles of Mo<sub>2</sub>C carbide (with a size of 5–30 nm) weakly modified by nickel (2–4 at.%) that are quickly deactivated in the course of the reaction becoming covered with a layer of graphite-like carbon with a thickness of about 5 nm. In the zeolite channels oxidized Mo-containing clusters (Mo<sup>5+</sup>) were found, their EDX analysis revealed the absence of Ni in their composition.

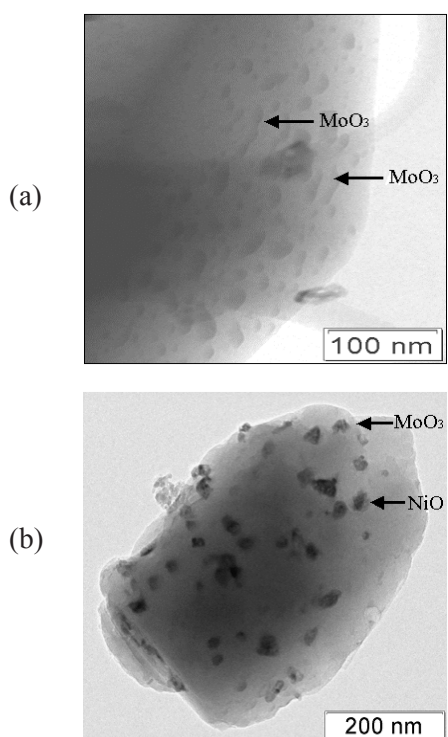


Fig. 4. HRTEM images of 0.1% Ni-4.0% Mo/ZSM-5 catalyst before the reaction: a – two-dimensional oxide particles; b – coarsely dispersed particles of MoO<sub>3</sub> and NiO [83].

The TEM images of the Ni-Mo/ZSM-5 catalyst show the presence of carbon threads with a diameter from 10 to 50 nm in the catalyst already after 10 min of its operation (Fig. 5). The amount of thread-like carbon substantially increases with the process duration. The carbon in the threads has a tubular or conical arrangement of graphite-like layers with metal particles located on the ends of the growing threads and also in the inner voids.

According to the data of EDX analysis, the average composition of the metal at the end of threads corresponds to Ni-Mo alloys with different compositions. For example, in particles with a size of ~10 nm, the atomic ratio Ni/Mo = 50/50, while in

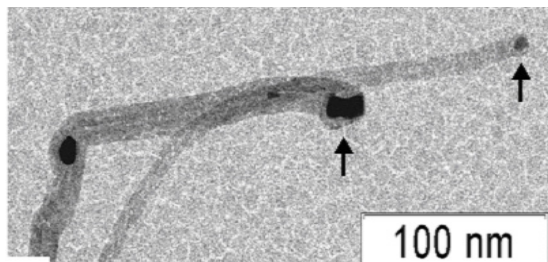


Fig. 5. TEM images of carbon threads in the catalyst 0.1% Ni-4.0% Mo/ZSM-5 after the reaction: metal particles are observed at the ends of the threads and in inner cavities [83].

larger particles (~30 nm) it is equal to 20/80 Small particles of inclusion inside the cavities torn from the back side of larger particles contain mainly Ni and an only small fraction of Mo. The particles of Ni-Mo alloy at the ends of the carbon threads are not deactivated for a long time. This is explained by the fact that the reaction proceeds at the active front part of particles not covered by carbon, while the thread growth occurs at its back side. Besides, such particles are transferred from the zeolite surface also subject to coking.

Thus, in Ni-Mo/ZSM-5 catalysts particles of different nature form: Mo clusters (with a size of ~1 nm) inside zeolite channels, molybdenum carbide particles (5–30 nm) on the outer zeolite surface, and particles of Ni-Mo alloy on which the growth of carbon threads occurs under the reaction conditions. The only small addition of Ni (0.1%) leads to the formation of the most stable catalyst. Larger Ni content results in much lower stability. As it follows from TEM and DTA data, with an increase of the Ni content in the zeolite the amount of the formed coke increases. According to the literature data [107, 108], the mass of the thread-like carbon formed on Ni-containing catalysts can exceed the mass of the zeolite by hundreds and thousands of times. It appears that the content of Ni exceeding the found optimum value of 0.1 wt.% causes the deactivation of the catalytic system due to the blocking of pores in the zeolite structure by thread-like carbon with the final formation of dense coke deposits.

The results of the study of the promoting effect of iron show that Mo/ZSM-5 samples modified by iron powder are characterized by higher activity and stability than those prepared by impregnation or mechanical mixing with iron oxide [85]. This is due to the highly dispersed state of Fe particles in the catalyst, which facilitates the formation of a large number of active sites on the catalyst surface. The addition of Fe NSP to the initial system increases its activity and stability. The most efficient 4.0% Mo/ZSM-5 catalyst is the one containing 0.1 wt.% Fe.

The study of the structure and composition of Fe-Mo-containing by HRTEM and EDX methods showed that the active centers for the reaction of methane dehydroaromatization were bimetal Fe-Mo particles [85]. In the composition of the catalyst containing 1 wt.% Fe NSP after 380 min of operation particles of Fe-Mo alloy with size from several to tens of nanometers were found (Fig. 6). Particles containing only iron or molybdenum

were not detected. In the course of the process, the formation of carbon threads with a tubular or conical arrangement of graphite-like layers takes place.

The mechanism of the formation of carbon threads on metals of iron sub-group and their alloys with other metals was studied in detail in the work [108]. It was shown that a particle of a metal or an alloy at the interaction with carbon catalyzes the carbon growth through the stage of the formation of metastable carbides on the active surface of the particle. The carbide decomposition produces metal and carbon atoms that diffuse to the back side of the particle where a graphite-like phase forms. According to this mechanism, the front surface of a metal or alloy particle retains the catalytic activity for a long time in spite of the carbon accumulation.

The particles of Fe-Mo alloy are located both on the surface of zeolite crystals and on the ends of rather thin carbon nanotubes (CNT) with a diameter of  $\sim 10$  nm filling the space between zeolite particles (Fig. 6). CNTs form during the process of methane dehydroaromatization separating particles of Fe-Mo from the surface of zeolite crystals. According to EDX data, Fe-Mo particles catalyzing the CNT growth usually contain no less than 50 at.% of iron. It is known that the formation of carbon in the form of CNT does not lead to catalyst deactivation because the active part of the catalyst surface at the ends of carbon nanotubes is not covered by carbon and is available for interacting molecules. The HRTEM pictures show that the structure of CNTs is rather regular with an empty channel of about 10 nm in diameter inside them (Fig. 7a). Part of CNTs has diameters of several tens of nanometers, with their structure highly distorted – up to the formation of spiral-like structures (Fig. 7b).

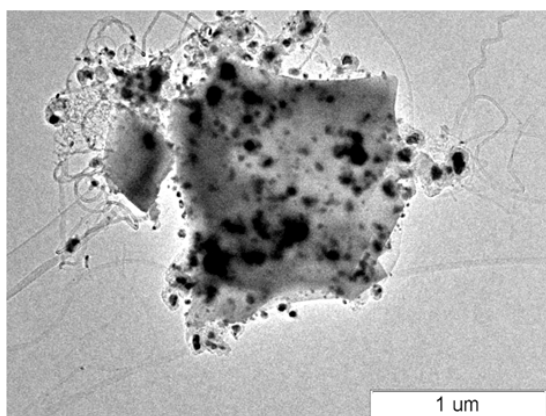


Fig. 6. Nanoparticles of Fe-Mo alloy located on the zeolite surface and separated from the surface by carbon nanotubes [85].

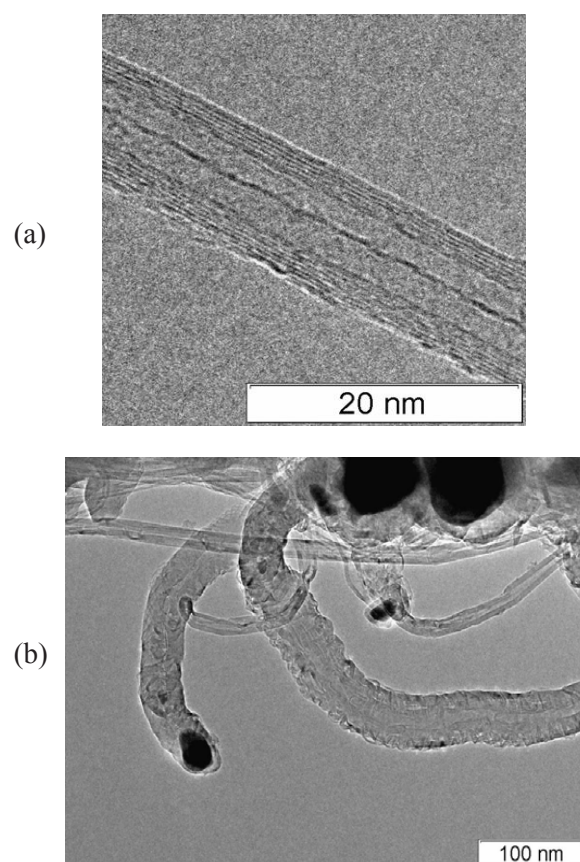


Fig. 7. The regular structure of a thin CNT (diameter  $\approx 10$  nm) (a) and distorted structures of thick CNTs (diameter 40–60 nm) (b) [85].

Simultaneously some fractions of Fe and Mo are found in the composition of “core-shell” structures consisting of Fe-Mo alloy and carbon layers completely shielding their surface (Fig. 8).

The size of such particles varies in a wide range (10–100 nm). It is apparent that Fe-Mo alloy in the composition of “core-shell” structures loses its activity during the methane conversion much faster because of their blocking by carbon already at the initial period of the reaction.

Thus, it can be noted that the reaction of methane dehydroaromatization in the presence of Fe-Mo/ZSM-5 proceeds most efficiently on bimetal nanoparticles of Fe-Mo alloy with a size 10 nm and less, having the composition  $\text{Fe:Mo} \approx 1:1$ . The deactivation of such particles does not occur in spite of the CNT growth on them. Particles with a larger size form “core-shell” structures, and they are deactivated by layers of carbon deposited on their surface.

The introduction of NSP of Ag (0.05–2.0%) into 4.0% Mo/ZSM-5 catalyst also leads to an increase in its activity and stability [84]. The highest values of the activity and stability are exhibited by

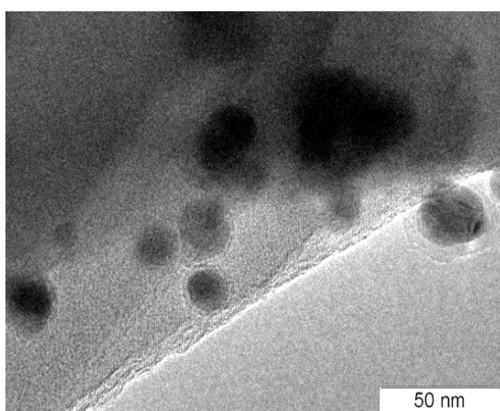


Fig. 8. «Core-shell» structure on the zeolite surface wherein the particles of Fe-Mo alloy are blocked by carbon [85].

the 4.0% Mo/ZSM-5 catalyst containing 0.1% Ag. With the growth of silver content in the catalytic system its dispersion changes because of the agglomeration of particles in the course of the reaction, which is accompanied by the blocking of the active  $\text{Mo}_2\text{C}$  surface centers and zeolite channels where oxide-like molybdenum clusters are located as well as the acid sites of the zeolite [109]. This is confirmed by HRTEM and EDX that indicate the presence of Ag in the composition of molybdenum carbide particles and also on aggregates of micron sizes.

Electron microscopy studies [84] show that the initial 0.1% Ag-4.0% Mo/ZSM-5 sample contains zeolite particles as a prevailing fraction and silver particles present as aggregates of micron sizes (Fig. 9). The particles of silver and zeolite are arranged without any signs of topochemical interaction with each other. Separate particles of Mo compounds were not detected. Only in some cases, nanoparticles with an increased contrast were found to exist on the zeolite surface that according to EDX spectra corresponded to a Mo compound. Also, EDX spectra recorded on zeolite regions free from surface particles contain the Mo signal, which allows the conclusion about the presence of molecularly dispersed oxidized species of Mo in the zeolite.

In the catalyst 0.1% Ag-4.0% Mo/ZSM-5 after 10 min operation in the methane dehydroaromatization process the uniform disperse distribution of molybdenum carbide particles over the zeolite surface is observed [84]. On the surface of these particles 5–10 nm in size, only thin graphene islands are seen with a thickness not exceeding, as a rule, two carbon monolayers. In the sample that worked for 380 min, a great number of three-dimensional  $\text{Mo}_2\text{C}$  particles were observed in close contact

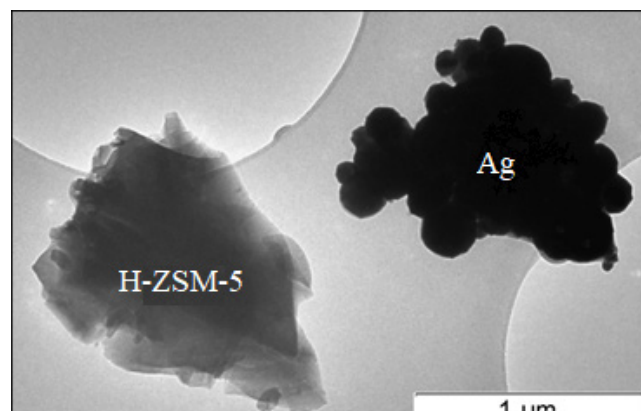


Fig. 9. The HRTEM image of zeolite and silver particles in the initial 0.1% Ag-4.0% Mo/ZSM-5 catalyst [84].

with the zeolite surface (Fig. 10a). The particles of Mo carbide (5–50 nm) are cut with the formation of elongated or flat forms. The HRTEM images of the crystal lattice and the two-dimensional Fourier picture with the identification of Mo carbide from the obtained reflexes are shown in Fig. 10b. After the reaction, individual silver particles were not found in the catalyst. According to EDX, silver is present in the composition of Mo carbide particles located on the zeolite surface. From the EDX data, it follows that the atomic ratio Ag:Mo is equal to 6:94. In the literature, many double compounds of Ag and Mo are described [84]. Apparently, the formation of a double compound containing oxidized forms of metals occurs in the gas phase at the sample thermal treatment at 750 °C for 380 min in the course of the reaction similarly to processes observed in the case of catalysts with the addition of NSP of Ni and Fe [83, 85].

As it was shown for the initial Mo/ZSM-5 catalyst, the EDX spectrum recorded on the zeolite regions free from three-dimensional  $\text{Mo}_2\text{C}$  particles contains the Mo signal. This is explained by the fact that the major part of Mo is located in the zeolite channels in the composition of oxide-like clusters (~1 nm), the nature of which was previously studied HRTEM and ESR methods [110]. It should be noted the Ag signal in these spectra is absent, i.e. the clusters do not contain silver. The absence of Ni and Fe in oxide-like clusters in the zeolite bulk was also observed at the modification of Mo/ZSM-5 catalyst with NSP of these metals. The EDX spectra of the 0.1% Ag-4.0% Mo/ZSM-5 sample after 2040 min of the reaction show the absence of even traces of Ag both on the surface particles and in the bulk. At the same time in the sample after 380 min operation, the inclusion of Ag in large Mo carbide particles located on the

zeolite surface is observed. Therefore the long operation of the catalyst in the reaction of methane dehydroaromatization leads to the removal of silver from Mo carbide particles.

Thus, the modification of Mo/ZSM-5 catalyst by silver increases its activity and the duration of the stable operation in the process of methane dehydroaromatization. The highest activity and stability are exhibited by Mo/ZSM-5 sample containing 0.1% NSP of Ag. An increase in the duration of the catalyst stable operation is connected with a decrease in the rate of the coke formation. By contrast to Ni-Mo/ZSM-5 and Fe-Mo/ZSM-5 catalysts [83, 85], the formation of thread-like carbon that can block the catalyst pores is not detected on the catalyst Ag-Mo/ZSM-5, which is the apparent explanation of the stability of this catalyst.

So it was established that the addition of small amounts (0.05–1 wt.%) of NSP of Fe, Ni, and Ag influences the activity, selectivity, and the resistance to coking of Mo/ZSM-5 catalysts. Using HR-

TEM, EDX, and ESR methods it was shown that the causes leading to an increase in the activity and stability owing to additions of different metals have different natures. In all studied samples the presence of oxidized Mo-containing clusters ( $\text{Mo}^{5+}$ ) with a size of ~1 nm inside the zeolite channels was observed, and, in the opinion of many researchers, these species act as the catalyst active sites [74, 81, 111, 112]. The presence of modifying additives can lead to an increase in the number of clusters inside the channels in Mo/ZSM-5 catalyst, which can promote the stable operation of the catalyst in the reaction of methane dehydroaromatization. When Ag NSP serves as a promoting additive, an enhanced duration of the catalyst stable operation is due to a decrease in the rate of the coke formation. In the case of NSP of Ni and Fe the formation of Ni-Mo and Fe-Mo alloys located at the ends of carbon threads is observed. The front surface of a metal or alloy particle retains the catalytic activity for a long time in spite of the carbon accumulation. Besides, the study of acid properties of the initial and metal-doped 4.0% Mo/ZSM-5 catalyst shows a change in the acidic characteristics that is most pronounced at high content of the promoters.

The greatest decrease in the strength and concentration of acid centers is observed at the Mo introduction into the zeolite, which points to its interaction with the acid centers in zeolite at its calcination during the catalyst preparation. The decrease of the sample acidity is caused by the Al withdrawal from the zeolite lattice during Mo/ZSM-5 catalyst calcination and the formation of the  $\text{Al}_2(\text{MoO}_4)_3$  crystal phase [113]. At the addition of 0.1% NSP of Fe, Ni, and Ag to 4.0% Mo/ZSM-5 catalyst an insignificant decrease in the concentration of acid centers of two types occurs. An increase in the metal content to 0.5–1.0% results in an increased concentration of the acid centers in the catalyst, however, their strength remains unchanged. The change in the acid properties of M-Mo-containing zeolites is connected with the creation of new active sites on their surface due to the formation of Me-Mo compounds with different stoichiometry at the interaction of Mo with metals.

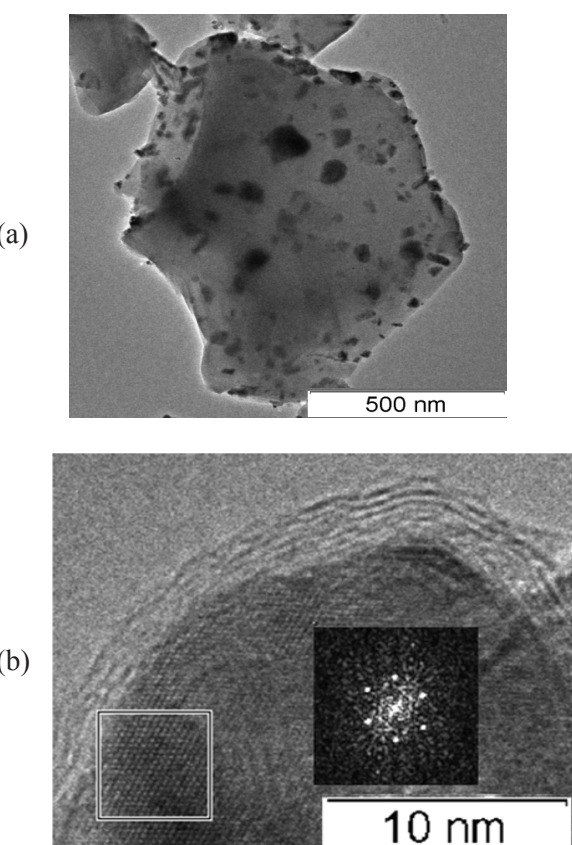


Fig. 10. HRTEM picture of the catalyst 0.1% Ag-4.0% Mo/ZSM-5 after 380 min of the methane dehydroaromatization reaction (a) and graphite-like layers on the surface of  $\text{Mo}_2\text{C}$  (b). The insert shows Fourier picture with reflexes from  $\text{Mo}_2\text{C}$  ( $d_{100} = 0.26 \text{ nm}$ ,  $d_{002} = 0.24 \text{ nm}$ ,  $d_{101} = 0.23 \text{ nm}$ ) and the corresponding region of the HRTEM image [84].

### 3. Reforming of hydrocarbon raw materials

The introduction of modifying additives into the composition of Ni catalyst is a rather wide-spread approach directed to the improvement of functional characteristics of catalysts developed for various catalytic processes (Fig. 11) [114–139].

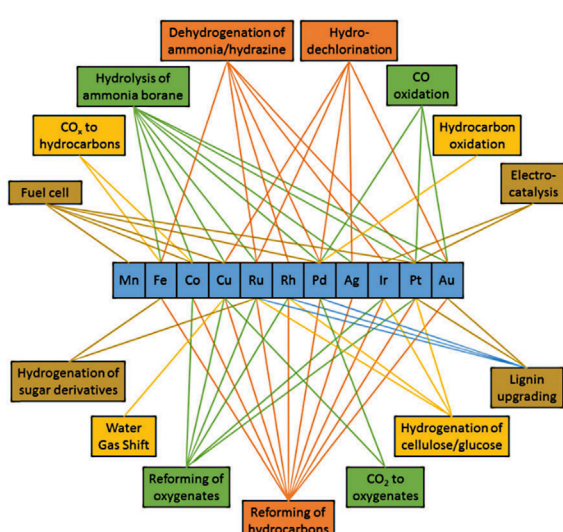


Fig. 11. Modifying additives (M) in the composition of bimetal catalysts NiM for various catalytic processes. Reproduced from Ref. [114] with permission from the Royal Society of Chemistry.

Various metals (Rh, Pd, Pt, Ir, Ru, Re, Mo, Mn, Sn, and Cu) can act as modifying additives to Ni catalysts for the reforming of hydrocarbon raw materials. Their content is varied in a wide range (0.07–2.8 wt.%).

The degree of the interaction between metals in the composition of bimetal catalysts is rather different, and it depends on the chemical composition of the catalyst, its preparation method, conditions of its activation and exploitation [115, 135]. In the case of the weak interaction between nickel and a modifying additive, the formation of monometal particles takes place, in the case of the strong interaction a surface or bulk alloy is formed (Fig. 12).

From literature analysis it follows that the presence of a noble metal 1) promotes the stabilization of the active component in a reduced state which decreases the probability of the catalyst deactivation caused by the oxidation of the active component [138, 139]; 2) decreases the rate of the formation of carbonaceous deposits [116], and 3) increases the catalyst resistance to sulfur compounds [117]. In addition to the change of redox

properties, the introduction of a second metal into the catalyst can affect the electronic structure [116] and dispersion [118] of the active component. For example, the presence of noble metals in the composition of Ni/ $\alpha$ -Al<sub>2</sub>O<sub>3</sub> catalyst influences the size of Ni metal particles [119]. At an increase of the content of Pd, Rh and Ru (from 0.07 to 0.2 wt.%) the average size of Ni increases from 15, 19, and 23 nm to 23, 27, and 25 nm, respectively. On the contrary, in the case of the elevation of the content of Pt, Ir, and Au (from 0.14 to 0.4 wt.%) the size of Ni particles is reduced from 23, 21, and 26 nm to 20, 15, and 16 nm, correspondingly. However, independent of the Ni particle size, a temperature decrease in the initial section of the catalyst bed is observed in the case of bimetal catalysts.

The comparative study of bimetal Ni-M/Al<sub>2</sub>O<sub>3</sub>-catalysts (M = Pd, Pt, Au, Ir, Rh or Ru) showed [119] that Pd is the most effective promoter that provides an enhancement of the Ni dispersion, increases the Ni<sup>2+</sup> capability to reduction and suppresses Ni<sup>0</sup> oxidation in the course of the reaction of methane steam reforming. Based on the EXAFS study it is concluded [119] that the improvement of the catalyst characteristics after Pd introduction is caused by the formation of Pd clusters interacting with Ni particles. In the case of Ni-M/CeZrO<sub>2</sub> catalyst (M = Pt, Pd, Fe, and Ag), the Ag additive was shown to be the most effective promoter Ag [126]. The higher activity and stability of Ni-Ag/CeZrO<sub>2</sub> catalyst in the reaction of methane autothermal reforming (ATR), in the authors' opinion, is due to its particular redox properties. It is revealed [121] that the activity of Ni-M/La<sub>2</sub>O<sub>3</sub> catalysts (M = Pt, Sn, Mo, Re, Pd) in the reaction ATR of CH<sub>4</sub> increases in the sequence: Pt < Sn < Mo < Re < Pd, which correlates with an increase of the reducibility of cations Ni<sup>n+</sup> in LaNi<sub>1-x</sub>M<sub>x</sub>O<sub>3</sub>.

The study of the catalytic activity and the temperature profile in the bed of Ni/Al<sub>2</sub>O<sub>3</sub> catalyst modified by different metals Pd, Pt, Au, Ir, Rh, and Ru in the oxidative steam reforming of methane showed [57, 119] that the catalyst modification inhibits the formation of overheated zones. It was

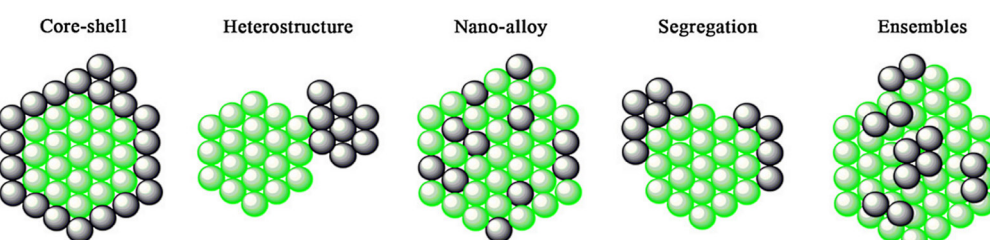


Fig. 12. Structures of bimetallic nanoparticles. Reproduced from Ref. [115] with permission from the Elsevier.

established that the most effective additive is Pd because even traces of palladium (0.07 wt.%) in the catalyst composition can provide a high rate of reduction and low rate of oxidation of Ni particles. It should be noted that the monometallic Pd catalysts do not exhibit any activity in the process of the oxidative steam reforming of methane.

The catalytic activity of Ni/CeO<sub>2</sub>-Al<sub>2</sub>O<sub>3</sub> and Ni/La<sub>2</sub>O<sub>3</sub>-Al<sub>2</sub>O<sub>3</sub> modified by noble metals (Pt, Ir, Pd, and Ru) in the processes of steam reforming of ethanol and glycerol was studied [56, 140]. The best result was achieved in the presence of Ni-Pd/CeO<sub>2</sub>-Al<sub>2</sub>O<sub>3</sub> and Ni-M/La<sub>2</sub>O<sub>3</sub>-Al<sub>2</sub>O<sub>3</sub> (M = Pd, Pt) catalysts at 600 °C in the reaction of ethanol steam reforming and on NiPt/CeO<sub>2</sub>-Al<sub>2</sub>O<sub>3</sub> catalyst at 700 °C in the reaction of glycerol steam reforming. The catalysts containing noble metals exhibited good stability and resistance to deactivation during the reaction. This agrees with the fact that the addition of modifying agents (0.1 and 0.3 wt.%) stabilizes Ni particles in the reduced state in reforming processes.

To increase the resistance of Pd catalysts of low-temperature methane oxidation to the inhibiting effect of water vapor up to 10% of metal oxide modifying agents were introduced into the catalyst composition [122]. A series of binary catalysts supported on cordierite monoliths PdO-M<sub>x</sub>O<sub>y</sub>/Al<sub>2</sub>O<sub>3</sub> (M = Co, Cu, Fe, Ni, Mn, and Sn) were studied. The results showed that the introduction of certain additives could increase the stability of Pd catalysts at rather high content of water vapor in the reaction mixture. Oxides of Co and Sn can serve as an effective additive, but the most positive effect is attained in the case of NiO [122]. The criteria of the conservation of the catalytic activity in the presence of water vapor were formulated. They are high crystallinity of the supported PdO, its uniform distribution over the surface of the modified Al<sub>2</sub>O<sub>3</sub>, and its weak interaction with the support components. This is provided by the deposition of the Pd precursor on the completely formed phase of the oxide modifier stable in the range of possible reactor temperatures (< 550 °C). At the optimum content of the oxide additive and the optimum mode of the introduction of NiO, Co<sub>3</sub>O<sub>4</sub> or SnO<sub>2</sub>, the deactivation of Pd catalysts under the action of water vapor can be completely excluded.

The study of catalysts Ni/Al<sub>2</sub>O<sub>3</sub> (15 wt.% Ni) modified by the addition of Re (0.5, 1, 2 and 3 wt.%) in the reaction of oxidative amination of monoethanolamine was described in [123]. It was found that the selectivity of the process increases significantly at an increase of the Re content to 2 wt.%. The cat-

alysts with Ni (15 wt.%) and Ni-Re (15 wt.% Ni and 2 wt.% Re) were studied in more detail. It was established that the Ni-Re/Al<sub>2</sub>O<sub>3</sub> samples exhibited higher activity, selectivity, and stability in comparison with the monometallic Ni/Al<sub>2</sub>O<sub>3</sub> catalyst. At the addition of Re, the fraction of active Ni<sup>0</sup> particles increases, the reducibility and acid properties of Ni-Re/Al<sub>2</sub>O<sub>3</sub> are improved. It was shown [123] that Re-containing clusters tend to the localization on the surface of NiO particles facilitating the stabilization of NiO in the reduced state and hindering the catalyst deactivation due to the sintering of the active component.

For the production of hydrogen-containing gas by the method of methane reforming with CO<sub>2</sub>, catalysts Ni/Al-Mg-O doped by Co, Cu, Mn or Zr were studied [124]. It was found that in the case of Ni-Co and Ni-Cu catalysts, the better distribution of the active component over the support surface was observed in comparison with the Ni sample. The Ni-Co sample had the highest dispersion of the active component among the studied catalysts. On the contrary, Ni-Zr and Ni-Mn samples were characterized by a lower dispersion of Ni. It was supposed that ZrO<sub>2</sub> and Mn<sub>2</sub>O<sub>3</sub> migrate to the surface of Ni particles decreasing the concentration of the active sites. The activity of the samples was shown to increase in the following series: Co>Cu>non-modified >Mn>Zn. It is established that the most important factors affecting the catalyst activity are the Ni dispersion and the reducibility of the active component. It is noted that Ni-Mn and Ni-Zr samples provide a high rate of the formation of carbonaceous deposits. As in the case of the Ni-Co/Al-Mg-O catalyst [124], the bimetallic catalyst 7Ni<sub>3</sub>Co/LaAl [125] has the high resistance to the sintering of the active component and coke formation due to the high dispersion of metals and strong interaction between the metals and the support.

A decrease in the formation rate of carbonaceous deposits in the process of carbon dioxide methane reforming was found at the doping of Ni/Al-Mg-O catalyst with Mn. It was supposed that the observed effect was due to a decrease in the size of NiO particles and the formation of the NiMn<sub>2</sub>O<sub>4</sub> phase [124]. The introduction of tin into the composition of the Ni/α-Al<sub>2</sub>O<sub>3</sub> catalyst also leads to the inhibition of the formation of carbonaceous deposits [127, 128]. It is surmised that a low quantity of tin (molar ratio Sn/Ni < 0.025) selectively deposited onto Ni particles is sufficient for the destruction of ensembles of the active sites of carbon formation [127]. Besides, tin promotes a change in the electronic state of the

active component [129]. This leads to changes in C- and O-chemistry on the surface of the Ni-Sn alloy with the consequent removal of coke in the form of CO and  $\text{CO}_2$  instead of the coke formation. The experimental data are in good agreement with the DFT calculations illustrating the inhibition of the graphite formation on the surface of the Ni-Sn alloy [130]. A similar mechanism was elucidated for the Re additive whose presence on the surface of the Ni-Re alloy destroys the extended ensembles of Ni centers (geometrical effect) and decreases the electron density on Ni atoms (electronic effect) in Ni-Re/SiO<sub>2</sub> catalysts [131]. At the modification by Mo, the decoration of Ni particles with MoO<sub>x</sub> clusters was observed, which resulted in a decrease in the degree of the catalyst coking [132].

It should be noted that the efficiency of modifying additives depends on the composition of the oxide matrix of the support and the method of the promoter introduction into the catalyst [57, 115, 141]. According to the literature data [57], the structure of bimetallic Ni-Pd particles depends on the impregnation method (Fig. 13). It was shown that the combined introduction of cations of nickel and palladium (Ni+Pd) promotes the formation of bimetallic particles with a more uniform Pd distribution, and as a consequence provides a lower surface Pd concentration. In the case of sequential impregnation (Pd/Ni) the formation of bimetallic particles with a high surface Pd concentration – Pd clusters on the surface of Ni particles takes place. At a higher surface Pd concentration the promoting effect, i.e., the resistance of the active component to oxidation and coking is more expressed.

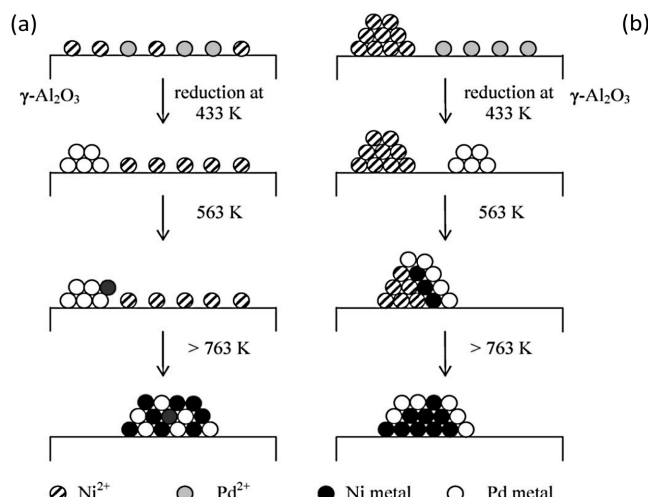


Fig. 13. Mechanism of the formation of bimetallic particles during catalyst synthesis by methods of combined (a) and sequential (b) impregnation. Reproduced from Ref. [57] with permission from the Elsevier.

In particular, it was found [142, 143] that in the case of 0.9Ni-0.1Pd/ $\gamma$ -Al<sub>2</sub>O<sub>3</sub> and 2.6Ni-0.1Pt/ $\gamma$ -Al<sub>2</sub>O<sub>3</sub> catalysts prepared by the method of sequential impregnation, as opposed to the combined impregnation, the enrichment of the surface of bimetallic particles with the metal-promoter occurred (M = Pd or Pt) providing the resistance of Ni-M particles to oxidation. However in the case of 10.6Ni-0.2Pd/ $\alpha$ -Al<sub>2</sub>O<sub>3</sub> catalyst [144], on the contrary, the combined impregnation leads to a higher surface concentration of Pd in the composition of bimetallic particles and better catalyst characteristics in the reaction of methane steam reforming.

The introduction of small amounts (0.07–0.4 wt.%) of noble metals into the catalyst composition is considered to be an effective method of prevention of overheated zones in the catalyst bed [56, 140, 144–146]. In [56], the comparative study of monometallic (10.6Ni, 0.14–0.4Pt, and 0.07–0.2Pd) and bimetallic (NiPt, NiPd) catalysts on  $\alpha$ -Al<sub>2</sub>O<sub>3</sub> in the oxidative steam reforming of methane was carried out. The bimetallic catalysts were prepared by methods of the combined Pd+Ni and Pt+Ni and sequential (Pt/Ni, Pd/Ni) impregnation. It was found that among monometallic catalysts the highest gradient in the catalyst bed was attained in the presence of Pt (0.14 wt.%) catalyst. The efficiency of bimetallic catalysts in the suppression of hot spot formation is higher than that of monometallic ones, and it depends both on the composition and preparation methods of catalysts, increasing in the series: Pd/Ni<Pt+Ni<Pd+Ni. It is supposed that the method of the introduction of the active component precursors influences the size of bimetal particles and the surface concentration of a noble metal, thus determining the resistance of Ni to oxidation and the concentration of the metallic Ni<sup>0</sup> in the course of the reaction.

On the contrary, the temperature gradient in the presence of Pd/Ni bimetallic catalysts on  $\gamma$ -Al<sub>2</sub>O<sub>3</sub> prepared by the method of sequential impregnation was much lower in comparison with Pd+Ni catalysts prepared by the method of combined impregnation. The Pd/Ni catalyst is considered more effective in the suppression of overheated zones owing to the presence of bimetallic particles with a higher Pd surface concentration than the particles in the composition of the Pd+Ni catalyst [142]. Thus an increase in the catalyst reducibility resulted in the prevention of hot spots in the catalyst bed in the reaction of methane ATR.

With the aim of development of an efficient catalyst for methane conversion into hydrogen-

containing gas, we studied the effect of the Pd content and the synthesis method (Ni+Pd combined impregnation, Pd/Ni sequential impregnation, Ni/Pd sequential impregnation) on physicochemical and catalytic properties of NiPd/CeZrO<sub>2</sub>/Al<sub>2</sub>O<sub>3</sub> [147]. It was shown that both the variation of the Pd content and the change of the method for introduction of the active component into the support matrix allow the regulation of redox properties of nickel cations but have no effect on the dispersion of NiO particles ( $14.0 \pm 0.5$  nm) and the catalyst phase composition (( $\gamma$ + $\delta$ )-Al<sub>2</sub>O<sub>3</sub>, solid solution CeZrO<sub>2</sub>, NiO). It was established that the activity of NiPd catalysts in the reaction of methane autothermal reforming depended on the synthesis method and increased in the following sequence: Ni+Pd<Ni/Pd<Pd/Ni. It was found that at a decrease of the Pd content in the composition NiPd/CeZrO<sub>2</sub>/Al<sub>2</sub>O<sub>3</sub> catalyst from 1 to 0.05 wt.%, the catalyst capability of self-activation and its high activity and stability in ATR of methane were retained. At 850 °C the hydrogen yield was ~70% at the methane conversion ~100% for 24 h time-on-stream.

The authors of this work also studied the influence of M=Pd, Pt, Re, Mo, Sn in the composition of Ni-M catalysts supported on La<sub>2</sub>O<sub>3</sub> or Ce<sub>0.5</sub>Zr<sub>0.5</sub>O<sub>2</sub>/Al<sub>2</sub>O<sub>3</sub> on their physicochemical properties and the activity [64, 121, 147]. The main physicochemical characteristics of these catalysts are given in Table 2 [64, 121]. It can be seen that catalysts on La<sub>2</sub>O<sub>3</sub> have the lowest values of the specific surface area (S<sub>BET</sub>). Their S<sub>BET</sub> only weakly depends on the type of the promoter, remaining in the range of 5–10 m<sup>2</sup>/g, which corresponds to typical values of S<sub>BET</sub> for such systems [148–151]. The specific surface area of samples based on Ce<sub>0.5</sub>Zr<sub>0.5</sub>O<sub>2</sub>/Al<sub>2</sub>O<sub>3</sub> is substantially higher (70–90 m<sup>2</sup>/g) with S<sub>BET</sub> values usually higher for bimetallic catalysts in comparison with the monometallic one, with the exclusion of the Sn-containing sample (Table 2).

According to the XRD data, samples of Ni-M/La<sub>2</sub>O<sub>3</sub> catalysts prepared by the citrate sol-gel method [121] are single-phase crystal systems represented by solid solutions with the perovskite structure. Despite certain differences between the efficient radius of Ni<sup>3+</sup> cation (0.56 Å) and the radii of cations-promoters (Pt<sup>4+</sup> – 0.63 Å, Pd<sup>2+</sup> – 0.86 Å, Re<sup>7+</sup> – 0.59 Å, Mo<sup>6+</sup> – 0.53 Å, Sn<sup>4+</sup> – 0.69 Å [152]), the parameters of the crystal lattice of LaNiO<sub>3</sub> are identical for all Ni-Me/La<sub>2</sub>O<sub>3</sub> catalysts (a = 5.468 ± 0.003, c = 6.588 ± 0.003). For Ni-M catalysts on Ce<sub>0.5</sub>Zr<sub>0.5</sub>O<sub>2</sub>/Al<sub>2</sub>O<sub>3</sub> support, the main phases are those of alumina (a mixture of phases

of  $\gamma$ - and  $\delta$ -Al<sub>2</sub>O<sub>3</sub>), a ceria-based solid solution, and also the phase of nickel oxide. In these samples, particles of nickel oxide with higher dispersion are formed [64]. The average size of NiO particles in Ni-M/Ce<sub>0.5</sub>Zr<sub>0.5</sub>O<sub>2</sub>/Al<sub>2</sub>O<sub>3</sub> is equal to ~10 nm. The XRD data agree well with the TEM results (Fig. 14) and 5D Operando Tomographic Diffraction [153]. The composition and dispersion of the Ni-containing phase are determined by the composition of the support. The presence of a promoting additive does not affect the structural characteristics of the active phase in samples before the reaction. For instance, for the catalyst Ni-M/La<sub>2</sub>O<sub>3</sub>, the main phase is that of mixed oxide La-Ni-O (Fig. 14a). In this case, the extreme variant of strong metal-support interaction is realized, i.e., the formation of the combined phase. In the catalysts Ni-M/<sub>10</sub>CeZrO<sub>2</sub>/Al<sub>2</sub>O<sub>3</sub>, particles of NiO are present on the surface of the support (Fig. 14b). Besides, in samples based on the Al-containing support, NiAl<sub>2</sub>O<sub>4</sub> particles with a size of ~10 nm are observed [50], which points to the

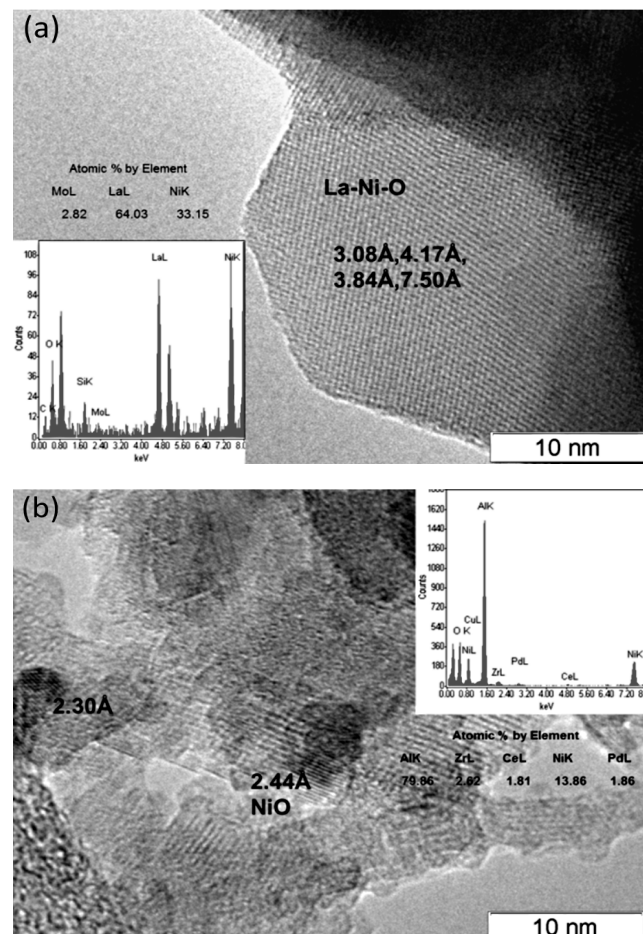


Fig. 14. Electron microscopic images of fresh Ni-Mo/La<sub>2</sub>O<sub>3</sub> (a) and Ni-Pd/<sub>10</sub>CeZrO<sub>2</sub>/Al<sub>2</sub>O<sub>3</sub> (b) catalysts [64, 121].

**Table 2**  
Physicochemical properties of catalysts [64, 121]

Promoter M	Content of Ni and promoter, wt. %	$S_{BET}$ , m <sup>2</sup> /g	Phase composition before and after the reaction	Size of particles NiO/Ni, nm	Maxima of TPR-H <sub>2</sub> peaks, °C	
					T <sub>1</sub>	T <sub>2</sub>
Ni-M/La <sub>2</sub> O <sub>3</sub> *						
Without promoter	25.7Ni	5	LaNiO <sub>3</sub> Ni, La <sub>2</sub> O <sub>3</sub>	-/30	340	520
Pt	24.0Ni, 0.62Pt	5	LaNiO <sub>3</sub> Ni, NiO, Pt, Pt <sub>3</sub> O <sub>4</sub> , La-Ni-O, La <sub>2</sub> O <sub>3</sub>	55/55	445	535
Pd	24.5Ni, 0.45Pd	6	LaNiO <sub>3</sub> Ni, La <sub>2</sub> O <sub>3</sub>	-/55	170	480
Re	24.4Ni, 0.66Re	9	LaNiO <sub>3</sub> Ni, La-Ni-O, Re clusters	-/55	400	545
Mo	23.0Ni, 0.44Mo	6	LaNiO <sub>3</sub> Ni, La-Ni-O	-/55	380	560
Sn	24.7Ni, 0.44Sn	5	LaNiO <sub>3</sub> Ni, NiO, La-Ni-O, La <sub>2</sub> O <sub>3</sub>	50/50	400	545
Ni-M/Ce <sub>0.5</sub> Zr <sub>0.5</sub> O <sub>2</sub> /Al <sub>2</sub> O <sub>3</sub> **						
Without promoter	9.9Ni	81	NiO, CeO <sub>2</sub> ***, ( $\gamma$ + $\delta$ )-Al <sub>2</sub> O <sub>3</sub> NiAl <sub>2</sub> O <sub>4</sub> , CeO <sub>2</sub>	10.0/- -	200	325
Pt	10.3Ni, 0.87Pt	87	NiO, CeO <sub>2</sub> , ( $\gamma$ + $\delta$ )-Al <sub>2</sub> O <sub>3</sub> NiO, Ni, CeO <sub>2</sub> , ( $\gamma$ + $\delta$ )-Al <sub>2</sub> O <sub>3</sub>	10.5/- 14.0/13.0	380	450
Pd	9.7Ni, 0.54Pd	89	NiO, CeO <sub>2</sub> , ( $\gamma$ + $\delta$ )-Al <sub>2</sub> O <sub>3</sub> Ni, CeO <sub>2</sub> , ( $\gamma$ + $\delta$ )-Al <sub>2</sub> O <sub>3</sub>	10.0/- -/17.0	130	400
Re	10.2Ni, 0.91Re	86	NiO, CeO <sub>2</sub> , ( $\gamma$ + $\delta$ )-Al <sub>2</sub> O <sub>3</sub> Ni, CeO <sub>2</sub> , ( $\gamma$ + $\delta$ )-Al <sub>2</sub> O <sub>3</sub>	11.0/- -/12.0	380	470
Mo	10.1Ni, 0.48Mo	83	NiO, CeO <sub>2</sub> , ( $\gamma$ + $\delta$ )-Al <sub>2</sub> O <sub>3</sub> NiO (traces), Ni, CeO <sub>2</sub> , ( $\gamma$ + $\delta$ )-Al <sub>2</sub> O <sub>3</sub>	11.0/- 17.0/0	-	505
Sn	9.6Ni, 0.57Sn	73	NiO, CeO <sub>2</sub> , ( $\gamma$ + $\delta$ )-Al <sub>2</sub> O <sub>3</sub> NiO (traces), NiAl <sub>2</sub> O <sub>4</sub> , CeO <sub>2</sub>	10.0/- -	360	430

\*Molar ratio M/Ni = 0.01. The phase composition of samples after the reaction was determined by HRTEM.

\*\*Molar ration M/Ni = 0.03. \*\*\*Solid solution based on ceria.

presence of strong metal-support interaction, as in the case of the La-Ni-O phase. As a rule, no separate phases containing promoters are observed in initial samples, which seems apparent because of the low content of the promoters (less than 1 wt.%).

As the stage of catalyst reduction with the formation of metal Ni<sup>0</sup> particles active in the reforming reactions is necessary for the catalyst activation, the prepared catalysts were studied by the method of the temperature-programmed reduction [50, 121, 147]. As can be seen from Table 2, the Ni cations reducibility evaluated from the TPR

peak positions depends on the promoter type. For the series of Ni-M/La<sub>2</sub>O<sub>3</sub> catalysts prepared with the variation of the promoter type, the Ni<sup>n+</sup> reducibility increases in the following sequence of the promoters: Pt<Sn~Re<Mo<Pd. As opposed to the lanthana-based catalyst in which the reduction of Ni<sup>n+</sup> is completed at ~700 °C, on Ni-M/10CeZrO<sub>2</sub>/Al<sub>2</sub>O<sub>3</sub> catalysts the reduction of Ni<sup>2+</sup> takes place in the lower temperature region (Table 2), finishing at 500–600 °C. As in the case of Ni-M/La<sub>2</sub>O<sub>3</sub>, for the series of Ni-M catalysts based on 10CeZrO<sub>2</sub>/Al<sub>2</sub>O<sub>3</sub>, the position of the main hydrogen absorption peak

depends on the promoter type and is usually found in the range of 325–525 °C (Table 2). It increases in the following order of M: Mo < Sn < Re ≤ Pd < Pt. The found dependences of Ni cation reducibility for samples on different supports:  $\text{La}_2\text{O}_3$  and  $10\text{CeZrO}_2/\text{Al}_2\text{O}_3$  are not identical which points to the important role of the support and different mechanisms of the promoter action. For Ni-M/ $\text{La}_2\text{O}_3$  only Pd additive improves the reducibility of Ni cations. The introduction of Pt, Mo, Re or Sn, on the contrary, shifts the process of Ni cation reduction to the high-temperature region, which can be connected with the effect of the stabilization of the perovskite structure described for the  $\text{LaNiO}_3$  perovskites promoted with Ru, Fe or Co [151, 154, 155]. The use of Ni catalysts with different redox properties of the active metal opens the possibility of regulating the characteristics of the reaction of methane autothermal reforming.

Figure 15 presents typical data on the temperature dependences of the ATR of  $\text{CH}_4$  reaction characteristics in the presence of non-promoted Ni catalysts. The main products of the reaction are  $\text{H}_2$ , CO and  $\text{CO}_2$ . It can be seen that with the temperature increase from 700 to 950 °C the methane conversion increases. This effect is most pronounced for lanthana-based catalysts. The oxygen conversion is equal to 100% in the studied temperature range. The hydrogen yield initially increases with the temperature rise, coming to a plateau. The most efficient are alumina-based systems, which is probably due to the higher specific surface area of the samples and the highly dispersed state of the active component (Table 2).

As can be seen from Fig. 16, in the low-temperature region, the hydrogen yield in ATR of  $\text{CH}_4$  in the presence of Ni-M/ $\text{La}_2\text{O}_3$  catalysts depends on the type of the promoter. An increase in the activity is observed in the following series of the promoters: Pt < Sn < Mo < Re < Pd. In the high-temperature region, the difference in the performance of the catalyst becomes insignificant (Fig. 16). Taking into consideration the same phase composition and insubstantial differences in the specific surface area of Ni-Me/ $\text{La}_2\text{O}_3$  catalysts it can be assumed that the observed dependence of the activity on the promoter type can be connected with differences in the reducibility of nickel cations in the studied samples (Table 2). As was noted above, the introduction of Pd in the catalyst composition leads to a substantial decrease in the temperature of  $\text{Ni}^{n+}$  reduction. After the activation of Ni/ $\text{La}_2\text{O}_3$  and Ni-Pd/ $\text{La}_2\text{O}_3$  catalyst under the reducing atmosphere

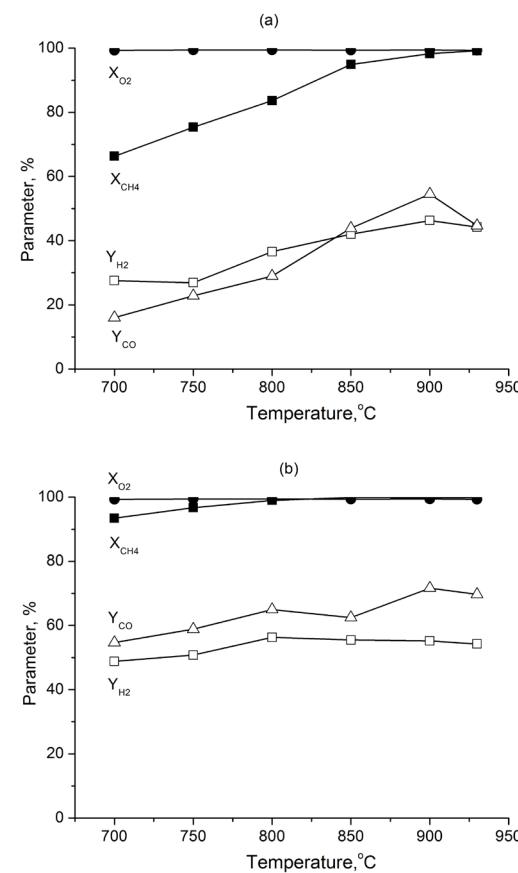


Fig. 15. The temperature dependences of the ATR  $\text{CH}_4$  reaction characteristics on the Ni/ $\text{La}_2\text{O}_3$  (a) and Ni/ $\text{Ce}_{0.5}\text{Zr}_{0.5}\text{O}_2/\text{Al}_2\text{O}_3$  (b) catalyst. Catalysts were previously activated at 800 °C in 30%  $\text{H}_2/\text{He}$  [147, 156].

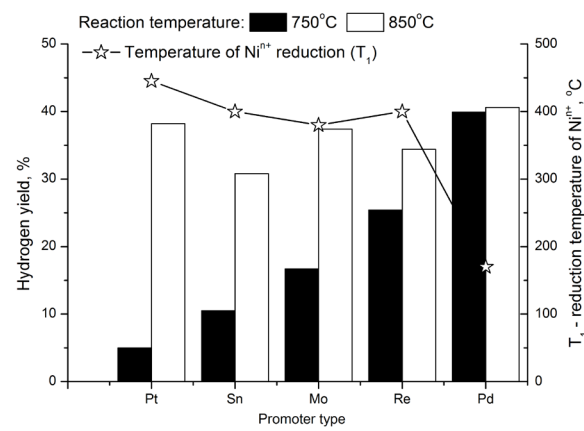


Fig. 16. Effect of promoter type in the composition of Ni-M/ $\text{La}_2\text{O}_3$  (M = Pt, Pd, Re, Mo, Sn) catalyst: hydrogen yield in ATR of  $\text{CH}_4$  reaction vs. reducibility of  $\text{Ni}^{n+}$  cations. The catalysts were previously activated at 800 °C in 30%  $\text{H}_2/\text{He}$  [121].

and the subsequent operation of the catalysts in the reaction, the destruction of the mixed oxide structure and the formation of the active  $\text{Ni}^0$  phase take place (Table 2). In the case of other additives,

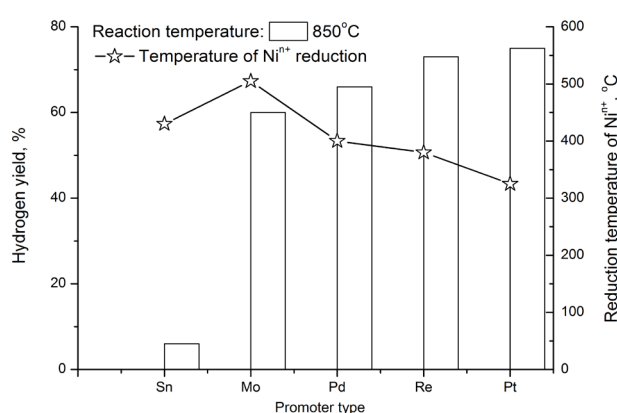


Fig. 17. Effect of promoter type in the composition of  $\text{Ni-M/Ce}_{0.5}\text{Zr}_{0.5}\text{O}_2/\text{Al}_2\text{O}_3$  ( $\text{M} = \text{Pt, Pd, Re, Mo, Sn}$ ) catalyst: hydrogen yield in ATR of  $\text{CH}_4$  reaction vs. reducibility of  $\text{Ni}^{2+}$  cations. The catalysts were tested without activation in  $\text{H}_2/\text{He}$  [64].

especially Pt, the mixed oxide structure is more resistant to the reduction, which leads to the worsening of the reducibility of Ni cations and prevents the stabilization of the active  $\text{Ni}^{\circ}$  phase in the course of the reaction.

Figure 17 presents the results of studying the activity of  $\text{Ni-M/Ce}_{0.5}\text{Zr}_{0.5}\text{O}_2/\text{Al}_2\text{O}_3$  catalysts in the reaction of methane ATR depending on the promoter type. It can be seen that the use of the additives Mo, Re, Pt or Pd provides high values of the  $\text{H}_2$  yield (65–75%) without their preliminary reduction [64]. The Ni-Sn catalyst is practically inactive in the reaction ATR  $\text{CH}_4$ . The analogous dependence is observed also for the non-modified Ni catalyst [147]. This Ni catalyst exhibits high activity after reduction, that however decreases with time [147]. It should be noted that the positive effect at the introduction of the additive of non-noble metal ( $\text{Re, M/Ni} = 0.03$ ) is analogous to that found at the introduction of noble metals (Pt, Pd) (Fig. 17). The average size of Ni-containing particles in samples after the reaction is equal to  $15 \pm 2 \text{ nm}$  (Table 2). The comparison of the size of particles of the Ni-containing phase before and after the reaction points to high resistance to sintering of the active component in the presence of modifying additives of Re or Pt. The highest resistance to oxidation is found for the samples modified by Pd or Re, which may be due to an alloy formation. The crystal cell parameter ( $a$ ) for  $\text{Ni}^{\circ}$  in  $\text{Ni-M}$  catalysts ( $\text{M} = \text{Pt, Pd, Re or Mo}$ ) is higher in comparison with the table value for  $\text{Ni}^{\circ}$  ( $a = 3.523 \text{ \AA}$ ):  $3.550 \text{ \AA}$  ( $\text{M} = \text{Pt}$ ),  $3.547 \text{ \AA}$  ( $\text{M} = \text{Pd}$ ),  $3.541 \text{ \AA}$  ( $\text{M} = \text{Re}$ ), and  $3.534 \text{ \AA}$  ( $\text{M} = \text{Mo}$ ) [64].

At  $850 \text{ }^{\circ}\text{C}$  in the reaction of ATR of  $\text{CH}_4$  in the presence of  $\text{Ni-0.9Re/Ce}_{0.5}\text{Zr}_{0.5}\text{O}_2/\text{Al}_2\text{O}_3$ , the hydrogen yield is equal to 70% that is close to the equilibrium value [48, 64]. The attained process indicators are comparable to or higher than those described in the literature [126, 157]. This allows us to consider the  $\text{Ni-0.9Re/Ce}_{0.5}\text{Zr}_{0.5}\text{O}_2/\text{Al}_2\text{O}_3$  catalyst as a promising catalytic system for the efficient conversion of methane into hydrogen-containing gas.

#### 4. Conclusion

The studies of non-oxidative methane conversion showed that the addition of small amounts (0.05–1.0 wt.%) of nanopowders of Fe, Ni, and Ag to Mo/ZSM-5 catalysts affected their activity and selectivity and also increased the duration of stable catalyst operation due to an increase in the resistance to coking. Using HRTEM, EDX, and ESR methods it was shown that the causes leading to an increase in the activity and stability owing to additions of different metals have different natures. In the case of NSP of Ni and Fe the formation of Ni-Mo and Fe-Mo alloys located at the ends of carbon threads is observed. The front surface of a metal or alloy particle retains the catalytic activity for a long time in spite of the carbon accumulation. When Ag NSP serves as a promoting additive, an enhanced duration of the catalyst stable operation is due to a decrease in the rate of the coke formation. In all studied samples the presence of oxidized Mo-containing clusters ( $\text{Mo}^{5+}$ ) with a size of  $\sim 1 \text{ nm}$  inside the zeolite channels was observed, these species act as the catalyst active sites. The presence of modifying additives can lead to an increase in the number of clusters inside the channels in the Mo/ZSM-5 catalyst, which can promote the stable operation of the catalyst in the reaction of methane dehydroaromatization.

Thus, the addition of a small amount of a second metal to a Mo-containing catalyst for methane dehydroaromatization promotes the improvement of its catalytic properties and therefore an increase in the efficiency of the process of direct conversion of natural gas (methane) into liquid products, which will serve as the basis for the development of a technology for methane processing into aromatic hydrocarbons.

The introduction of modifying additives is an efficient approach to an increase in the activity and stability of Ni reforming catalysts. Usually, noble metals (Pt, Pd, Rh, Ir, Ru) are used as promoters,

and their positive effect is based on the improvement of the reducibility of particles containing  $\text{Ni}^{2+}$  ions. While noble metals act as efficient promoters, their use is rather limited due to their high price. Therefore the urgent task is the development of an economically advantageous bimetallic catalyst providing high values of activity and stability in processes of methane conversion. The alternative additives are non-noble metals (Co, Cu, Mn, Re, Mo, Sn). Their promoting effect is connected with a change of the redox properties of  $\text{Ni}^{2+}$  and/or the character of the metal-support interaction and the inhibition of the coke formation. The variation of the method of introduction of a modifying additive allows the regulation of its distribution in the sample matrix and the degree of its interaction with Ni, which will determine the structure of bimetallic particles (segregation, ensembles, core-shell or alloy) and their functional properties. The degree of the interaction nickel-promoter, mechanism of the action of a modifying additive and its optimum content depend on the catalyst composition and process conditions.

The comparative analysis of the effect of noble ( $M = \text{Pt}, \text{Pd}$ ) and non-noble ( $M = \text{Re}, \text{Mo}, \text{Sn}$ ) additives in Ni-M catalysts for methane autothermal reforming on their physicochemical and catalytic properties allowed the elucidation of the optimum composition of bimetallic catalyst – Ni-0.9Re/ $\text{Ce}_{0.5}\text{Zr}_{0.5}\text{O}_2/\text{Al}_2\text{O}_3$ . This catalyst under conditions of the methane ATR reaction is capable of self-activation, it is resistant to oxidation and sintering of the active component and coking. The activity and stability of this catalyst are comparable to those of catalysts modified by noble metals.

## Acknowledgments

This work was performed as part of the state assignments of the Institute of Catalysis, Siberian Branch, Russian Academy of Sciences (project AAAA-A21-121011490008-3) and the Institute of Petroleum Chemistry, Siberian Branch, Russian Academy of Sciences (project 0295-2021-0004).

## References

- [1]. C.P.S. Badenhorst, U.T. Bornscheuer, *Trends Biochem. Sci.* 43 (2018) 180–198. DOI: [10.1016/j.tibs.2018.01.003](https://doi.org/10.1016/j.tibs.2018.01.003)
- [2]. T. Palmer, P.L. Bonner. Enzymes: Biochemistry, Biotechnology, Clinical Chemistry, 2<sup>nd</sup> Edition, 2007.
- [3]. Catalysts, Petroleum and Chemical Process. [Electronic Resource]. <https://ihsmarkit.com/products/chemical-catalysts-petroleum-and-chemical-scup.html> (accessed 01.02.2021)
- [4]. Z. Xie, Z. Liu, Y. Wang, Z. Jin, *Nat. Sci. Rev.* 2 (2015) 167–182. DOI: [10.1093/nsr/nwv019](https://doi.org/10.1093/nsr/nwv019)
- [5]. C.R. Catlow, M. Davidson, C. Hardacre, G.J. Hutchings, *Philos. Trans. R. Soc. A Math. Phys. Eng. Sci.* 374 (2016) 20150089. DOI: <http://doi.org/10.1098/rsta.2015.0089>
- [6]. M. Beller, G. Centi, *ChemSusChem* 2 (2009) 459–460. DOI: [10.1002/cssc.200900118](https://doi.org/10.1002/cssc.200900118)
- [7]. C.H. Bartholomew, R.J. Farrauto. Fundamentals of Industrial Catalytic Processes: 2<sup>nd</sup> Edition, John Wiley and Sons, 2010.
- [8]. Catalyst Market. [Electronic Resource]. <https://www.alliedmarketresearch.com/catalysts-market> (accessed 01.02.2021)
- [9]. V.S. Arutyunov, O.V. Krylov, *Russ. Chem. Rev.* 74 (2005) 1111–1137. DOI: [10.1070/RC2005v074n12ABEH001199](https://doi.org/10.1070/RC2005v074n12ABEH001199)
- [10]. E. Tezel, H.E. Figen, S.Z. Baykara, *Int. J. Hydrogen Energ.* 44 (2019) 9930–9940. DOI: [10.1016/j.ijhydene.2018.12.151](https://doi.org/10.1016/j.ijhydene.2018.12.151)
- [11]. A. Holmen, *Catal. Today* 142 (2009) 2–8. DOI: [10.1016/j.cattod.2009.01.004](https://doi.org/10.1016/j.cattod.2009.01.004)
- [12]. J.J. Spivey, G. Hutchings, *Chem. Soc. Rev.* 43 (2014) 792–803. DOI: [10.1039/C3CS60259A](https://doi.org/10.1039/C3CS60259A)
- [13]. Z.R. Ismagilov, L.T. Tsikoza, E.V. Matus, G.S. Litvak, I.Z. Ismagilov, O.B. Sukhova, *Eurasian Chem.-Technol. J.* 7 (2005) 115–121. DOI: [10.18321/ectj622](https://doi.org/10.18321/ectj622)
- [14]. E.V. Matus, I.Z. Ismagilov, O.B. Sukhova, V.I. Zaikovskii, L.T. Tsikoza, Z.R. Ismagilov, J.A. Moulijn, *Ind. Eng. Chem. Res.* 46 (2007) 4063–4074. DOI: [10.1021/ie0609564](https://doi.org/10.1021/ie0609564)
- [15]. C. Brady, Q. Debruyne, A. Majumder, B. Goodfellow, R. Lobo, T. Calverley, B. Xu, *Chem. Eng. J.* 406 (2021) 127168. DOI: [10.1016/j.cej.2020.127168](https://doi.org/10.1016/j.cej.2020.127168)
- [16]. N. Kosinov, F.J.A.G. Coumans, E.A. Uslamin, A.S.G. Wijpkema, B. Mezari, E.J.M. Hensen, *ACS Catal.* 7 (2017) 520–529. DOI: [10.1021/acscatal.6b02497](https://doi.org/10.1021/acscatal.6b02497)
- [17]. C. Karakaya, H. Zhu, R.J. Kee, *Chem. Eng. Sci.* 123 (2015) 474–486. DOI: [10.1016/j.ces.2014.11.039](https://doi.org/10.1016/j.ces.2014.11.039)
- [18]. E. Yaghinirad, H. Aghdasinia, A. Naghizadeh, A. Niaezi, *Iran. J. Catal.* 9 (2019) 147–154.
- [19]. R. Horn, R. Schlögl, *Catal. Lett.* 145 (2015) 23–39. DOI: [10.1007/s10562-014-1417-z](https://doi.org/10.1007/s10562-014-1417-z)
- [20]. C.H.L. Tempelman, X. Zhu, E.J.M. Hensen, *Chinese J. Catal.* 36 (2015) 829–837. DOI: [10.1016/S1872-2067\(14\)60301-6](https://doi.org/10.1016/S1872-2067(14)60301-6)
- [21]. Z.R. Ismagilov, E.V. Matus, I.Z. Ismagilov, M.A. Kerzhentsev, V.I. Zailovskii, K.D. Dosumov, A.G. Mustafinc, *Eurasian Chem.-Technol. J.* 12 (2010) 9–16. DOI: [10.18321/ectj20](https://doi.org/10.18321/ectj20)

- [22]. E.V. Matus, O.B. Sukhova, I.Z. Ismagilov, L.T. Tsikoza, Z.R. Ismagilov, *React. Kinet. Catal. Lett.* 98 (2009) 59–67. DOI: 10.1007/s11144-009-0080-7
- [23]. Z.R. Ismagilov, E.V. Matus, L.T. Tsikoza, *Energy Environ. Sci.* 1 (2008) 526–541. DOI: 10.1007/s11144-009-0080-7
- [24]. Z. Zakaria, S.K. Kamarudin, *Renew. Sustain. Energy Rev.* (2016) 250–261. DOI: 10.1016/j.rser.2016.05.082
- [25]. B. Michalkiewicz, *Appl. Catal. A Gen.* 277 (2004) 147–153. DOI: 10.1016/j.apcata.2004.09.005
- [26]. L.D. Nguyen, S. Lordinat, H. Launay, A. Pigamo, J.L. Dubois, J.M.M. Millet, *J. Catal.* 237 (2006) 38–48. DOI: 10.1016/j.jcat.2005.10.016
- [27]. Y.A. Treger, V.N. Rozanov, *Rev. J. Chem.* 6 (2016) 83–123. DOI: 10.1134/S2079978016010039
- [28]. W. Yang, H. Wang, X. Zhu, L. Lin, *Top. Catal.* 35 (2005) 155–167. DOI: 10.1007/s11244-005-3820-6
- [29]. T. Fini, G. Patz, R. Wentzel, “Oxidative Coupling of Methane to Ethylene” (2014). [Electronic Resource]. [https://repository.upenn.edu/cgi/viewcontent.cgi?article=1064&context=cbe\\_sdr](https://repository.upenn.edu/cgi/viewcontent.cgi?article=1064&context=cbe_sdr) (accessed 01.02.2021)
- [30]. P. Tang, Q. Zhu, Z. Wu, D. Ma, *Energy Environ. Sci.* 7 (2014) 2580–2591. DOI: 10.1039/C4EE00604F
- [31]. I.Z. Ismagilov, E.V. Matus, V.S. Popkova, V.V. Kuznetsov, V.A. Ushakov, S.A. Yashnik, I.P. Prosvirin, M.A. Kerzhentsev, Z.R. Ismagilov, *Kinet. Catal.* 58 (2017) 622–629. DOI: 10.1134/S0023158417050068
- [32]. A. Shubin, I. Zilberberg, I. Ismagilov, E. Matus, M. Kerzhentsev, Z. Ismagilov, *Mol. Catal.* 445 (2018) 307–315. DOI: 10.1016/j.mcat.2017.11.039
- [33]. I.Z. Ismagilov, E.V. Matus, V.V. Kuznetsov, M.A. Kerzhentsev, S.A. Yashnik, T.V. Larina, I.P. Prosvirin, R.M. Navarro, J.L.G. Fierro, G. Gerritsen, H.C.L. Abbenhuis, Z.R. Ismagilov, *Eurasian Chem.-Technol. J.* 18 (2016) 93–110. DOI: 10.18321/ectj430
- [34]. I.Z. Ismagilov, E.V. Matus, S.D. Vasil'ev, V.V. Kuznetsov, M.A. Kerzhentsev, Z.R. Ismagilov, *Kinet. Catal.* 56 (2015) 456–465. DOI: 10.1134/S0023158415040096
- [35]. I.Z. Ismagilov, E.V. Matus, M.A. Kerzhentsev, I.P. Prosvirin, R.M. Navarro, J.L.G. Fierro, G. Gerritsen, E. Abbenhuis, Z.R. Ismagilov, *Eurasian Chem.-Technol. J.* 17 (2015) 105–118. DOI: 10.18321/ectj201
- [36]. S. Lee, Methane and its Derivatives. CRC Press, New York, USA, 2019. p. 424.
- [37]. J.R. Rostrup-Nielsen, *J. Catal.* 31 (1973) 173–199. DOI: 10.1016/0021-9517(73)90326-6
- [38]. V.S. Arutunov, O.V. Krylov, Oxidative Conversion of Methane, Nauka, Moscow, 1998.
- [39]. C.J. Liu, J. Ye, J. Jiang, Y. Pan, *ChemCatChem* 3 (2011) 529–541. DOI: 10.1002/cctc.201000358
- [40]. J.R. Rostrup-Nielsen, *Catal. Today* 71 (2002) 243–247. DOI: 10.1016/S0920-5861(01)00454-0
- [41]. N. Laosiripojana, S. Assabumrungrat, *Appl. Catal. A Gen.* 290 (2005) 200–211. DOI: 10.1016/j.apcata.2005.05.026
- [42]. F. Pompeo, N.N. Nichio, M.M.V.M. Souza, D.V. Cesar, O.A. Ferretti, M. Schmal, *Appl. Catal. A Gen.* 316 (2007) 175–183. DOI: 10.1016/j.apcata.2006.09.007
- [43]. K.C. Mondal, V.R. Choudhary, U.A. Joshi, *Appl. Catal. A Gen.* 316 (2007) 47–52. DOI: 10.1016/j.apcata.2006.09.016
- [44]. T. Utaka, S.A. Al-Drees, J. Ueda, Y. Iwasa, T. Takeuchi, R. Kikuchi, K. Eguchi, *Appl. Catal. A Gen.* 247 (2003) 125–131. DOI: 10.1016/S0926-860X(03)00129-7
- [45]. F. Mueller-Langer, E. Tzimas, M. Kaltschmitt, S. Petreves, *Int. J. Hydrogen Energ.* 32 (2007) 3797–3810. DOI: 10.1016/j.ijhydene.2007.05.027
- [46]. N.Z. Muradov, T.N. Veziroğlu, *Int. J. Hydrogen Energ.* 33 (2008) 6804–6839. DOI: 10.1016/j.ijhydene.2008.08.054
- [47]. M. Wietschel, M. Ball. The Hydrogen Economy Opportunities and Challenges, 2009, 613–639. DOI: 10.1017/CBO9780511635359.022
- [48]. I.Z. Ismagilov, E.V. Matus, V.V. Kuznetsov, M.A. Kerzhentsev, S.A. Yashnik, I.P. Prosvirin, N. Mota, R.M. Navarro, J.L.G. Fierro, Z.R. Ismagilov, *Int. J. Hydrogen Energ.* 39 (2014) 20992–21006. DOI: 10.1016/j.ijhydene.2014.10.044
- [49]. M.C. Alvarez-Galvan, N. Mota, M. Ojeda, S. Rojas, R.M. Navarro, J.L.G. Fierro, *Catal. Today* 171 (2011) 15–23. DOI: 10.1016/j.cattod.2011.02.028
- [50]. I.Z. Ismagilov, E.V. Matus, D.V. Nefedova, V.V. Kuznetsov, S.A. Yashnik, M.A. Kerzhentsev, Z.R. Ismagilov, *Kinet. Catal.* 56 (2015) 394–402. DOI: 10.1134/S0023158415030064
- [51]. Z.R. Ismagilov, E.V. Matus, I.Z. Ismagilov, O.B. Sukhova, S.A. Yashnik, V.A. Ushakov, M.A. Kerzhentsev, *Catal. Today* 323 (2019) 166–182. DOI: 10.1016/j.cattod.2018.06.035
- [52]. I.Z. Ismagilov, E.V. Matus, V.V. Kuznetsov, S.A. Yashnik, M.A. Kerzhentsev, G. Gerritsen, H.C.L. Abbenhuis, Z.R. Ismagilov, *Eurasian Chem.-Technol. J.* 19 (2017) 3–16. DOI: 10.18321/ectj497
- [53]. T.V. Choudhary, E. Aksoylu, D.W. Goodman, *Catal. Rev. Sci. Eng.* 45 (2003) 151–203. DOI: 10.1081/CR-120017010
- [54]. F. Jiao, J.J. Li, X. Pan, J. Xiao, H. Li, H. Ma, M. Wei, Y. Pan, Z. Zhou, M. Li, S. Miao, J.J. Li, Y. Zhu, D. Xiao, T. He, J. Yang, F. Qi, Q. Fu, X. Bao, *Science* 351 (2016) 1065–1068. DOI: 10.1126/science.aaf1835

- [55]. M. Wang, T. Zhao, M. Li, H. Wang, *RSC Adv.* 7 (2017) 41847–41854. DOI: 10.1039/C7RA08422F
- [56]. L.P.R. Profeti, J.A.C. Dias, J.M. Assaf, E.M. Assaf, *J. Power Sources* 190 (2009) 525–533. DOI: 10.1016/j.jpowsour.2008.12.104
- [57]. D. Li, Y. Nakagawa, K. Tomishige, *Appl. Catal. A Gen.* 408 (2011) 1–24. DOI: 10.1016/j.apcata.2011.09.018
- [58]. U. Menon, M. Rahman, S.J. Khatib, *Appl. Catal. A Gen.* 608 (2020) 117870. DOI: 10.1016/j.apcata.2020.117870
- [59]. D. Sun, Y. Du, Z. Wang, J. Zhang, Y. Li, J. Li, L. Kou, C. Li, J. Li, H. Feng, J. Lu, *Int. J. Hydrogen Energ.* 45 (2020) 16421–16431. DOI: 10.1016/j.ijhydene.2020.04.126
- [60]. V. Ramasubramanian, H. Ramsurn, G.L. Price, *Int. J. Hydrogen Energ.* 45 (2020) 12026–12036. DOI: 10.1016/j.ijhydene.2020.02.170
- [61]. S. Chen, J. Zaffran, B. Yang, *ACS Catal.* 10 (2020) 3074–3083. DOI: 10.1021/acscatal.9b04429
- [62]. O. Mohan, Shambhawi, A.A. Lapkin, S.H. Mushrif, *Catal. Sci. Technol.* 10 (2020) 6628–6643. DOI: 10.1039/D0CY00939C
- [63]. G.E. Ergazieva, M.M. Telbayeva, A.N. Popova, Z.R. Ismagilov, K. Dossumov, L.K. Myltykbayeva, V.G. Dodonov, S.A. Sozinov, A.I. Niyazbayeva, *Chem. Pap.* 75 (2021) 2765–2774. DOI: 10.1007/s11696-021-01516-y
- [64]. E.V. Matus, I.Z. Ismagilov, S.A. Yashnik, V.A. Ushakov, I.P. Prosvirin, M.A. Kerzhentsev, Z.R. Ismagilov, *Int. J. Hydrogen Energ.* 45 (2020) 33352–33369. DOI: 10.1016/j.ijhydene.2020.09.011
- [65]. D. Ma, W. Zhang, Y. Shu, X. Liu, Y. Xu, X. Bao, *Catal. Lett.* 66 (2000) 155–160. DOI: 10.1023/A:1019099607029
- [66]. F. Solymosi, J. Cserényi, A. Szöke, T. Bánsági, A. Oszkó, *J. Catal.* 165 (1997) 150–161. DOI: 10.1006/jcat.1997.1478
- [67]. Y. Xu, S. Liu, X. Guo, L. Wang, M. Xie, *Catal. Lett.* 30 (1995) 135–149. DOI: 10.1007/BF00813680
- [68]. X. Liu, Y. Xu, S-T. Wong, L. Wang, L. Qiu, N. Yang, *J. Mol. Catal. A Chem.* 120 (1997) 257–265. DOI: 10.1016/S1381-1169(96)00427-X
- [69]. Y. Xu, Y. Shu, S. Liu, J. Huang, X. Guo, *Catal. Lett.* 35 (1995) 233–243. DOI: 10.1007/BF00807179
- [70]. V. Ramasubramanian, H. Ramsurn, G.L. Price, *J. Energy Chem.* 34 (2019) 20–32. DOI: 10.1016/j.jecchem.2018.09.018
- [71]. A. López-Martín, A. Caballero, G. Colón, *Mol. Catal.* 486 (2020) 110787. DOI: 10.1016/j.mcat.2020.110787
- [72]. S.J. Han, S.K. Kim, A. Hwang, S. Kim, D.Y. Hong, G. Kwak, K.W. Jun, Y.T. Kim, *Appl. Catal. B Environ.* 241 (2019) 305–318. DOI: 10.1016/j.apcatb.2018.09.042
- [73]. B.M. Weckhuysen, D. Wang, M.P. Rosyne, J.H. Lunsford, *J. Catal.* 175 (1998) 338–346. DOI: 10.1006/jcat.1998.2010
- [74]. W. Ding, S. Li, G.D. Meitzner, E. Iglesia, *J. Phys. Chem. B* 105 (2001) 506–513. DOI: 10.1021/jp0030692
- [75]. L. Chen, J. Lin, H.C. Zeng, K.L. Tan, *Catal. Commun.* 2 (2001) 201–206. DOI: 10.1016/S1566-7367(01)00032-2
- [76]. O.V. Sedel'nikova, A.A. Stepanov, V.I. Zaikovskii, L.L. Korobitsyna, A.V. Vosmerikov, *Kinet. Catal.* 58 (2017) 51–57. DOI: 10.1134/S0023158417010074
- [77]. M. Nagai, T. Nishibayashi, S. Omi, *Appl. Catal. A-Gen.* 253 (2003) 101–112. DOI: 10.1016/S0926-860X(03)00529-5
- [78]. H. Liu, X. Bao, Y. Xu, *J. Catal.* 239 (2006) 441–450. DOI: 10.1016/j.jcat.2006.02.018
- [79]. D. Ma, Y. Shu, X. Bao, Y. Xu, *J. Catal.* 189 (2000) 314–325. DOI: 10.1006/jcat.1999.2704
- [80]. D. Wang, J.H. Lunsford, M.P. Rosyne, *J. Catal.* 169 (1997) 347–358. DOI: 10.1006/jcat.1997.1712
- [81]. H. Liu, W. Shen, X. Bao, Y. Xu, *Appl. Catal. A Gen.* 295 (2005) 79–88. DOI: 10.1016/j.apcata.2005.08.011
- [82]. S. Ma, X. Guo, L. Zhao, S. Scott, X. Bao, *J. Energy Chem.* 22 (2013) 1–20. DOI: 10.1016/S2095-4956(13)60001-7
- [83]. A.V. Vosmerikov, V.I. Zaikovskii, L.L. Korobitsyna, G.V. Echevskii, V.V. Kozlov, Y.E. Barbashin, S.P. Zhuravkov, *Kinet. Catal.* 50 (2009) 725–733. DOI: 10.1134/S0023158409050140
- [84]. A.V. Vosmerikov, V.I. Zaikovskii, L.L. Korobitsyna, V.V. Kozlov, N.V. Arbuzova, S.P. Zhuravkov, *Kinet. Catal.* 52 (2011) 427–433. DOI: 10.1134/S0023158411030190
- [85]. A.V. Vosmerikov, L.L. Korobitsyna, V.I. Zaikovskii, *J. Chem. Eng. Chem. Res.* 1 (2014) 205–212.
- [86]. S. Burns, J.S.J. Hargreaves, P. Pal, K.M. Parida, S. Parija, *Catal. Today* 114 (2006) 383–387. DOI: 10.1016/j.cattod.2006.02.030
- [87]. V. Abdelsayed, D. Shekhawat, M.W. Smith, *Fuel* 139 (2015) 401–410. DOI: 10.1016/j.fuel.2014.08.064
- [88]. V. Fila, M. Bernauer, B. Bernauer, Z. Sobalik, *Catal. Today* 256 (2015) 269–275. DOI: 10.1016/j.cattod.2015.02.035
- [89]. T. Kubota, N. Oshima, Y. Nakahara, M. Yanagimoto, Y. Okamoto, *J. Jpn. Petrol. Inst.* 49 (2006) 127–133. DOI: 10.1627/jpi.49.127
- [90]. S. Qi, B. Yang, *Catal. Today* 98 (2004) 639–645. DOI: 10.1016/j.cattod.2004.09.049
- [91]. A.K. Aboul-Gheit, A.E. Awadallah, A.A. Abouleinein, A.-L.H. Mahmoud, *Fuel* 90 (2011) 3040–3046. DOI: 10.1016/j.fuel.2011.05.010

- [92]. M.V. Luzgin, V.A. Rogov, S.S. Arzumanov, A. V. Toktarev, A.G. Stepanov, V.N. Parmon, *Catal. Today* 144 (2009) 265–272. DOI: [10.1016/j.cattod.2008.08.043](https://doi.org/10.1016/j.cattod.2008.08.043)
- [93]. B. Liu, Y. Yang, A. Sayari, *Appl. Catal. A Gen.* 214 (2001) 95–102. DOI: [10.1016/S0926-860X\(01\)00470-7](https://doi.org/10.1016/S0926-860X(01)00470-7)
- [94]. B.S. Liu, L. Jiang, H. Sun, C.T. Au, *Appl. Surf. Sci.* 253 (2007) 5092–5100. DOI: [10.1016/j.apsusc.2006.11.031](https://doi.org/10.1016/j.apsusc.2006.11.031)
- [95]. Y. Zhang, D. Wang, J. Fei, X. Zheng, *Aust. J. Chem.* 55 (2002) 531–534. DOI: [10.1071/CH01170](https://doi.org/10.1071/CH01170)
- [96]. M.W. Ngobeni, A.F. Carley, M.S. Scurrell, C.P. Nicolaides, *J. Mol. Catal. A Chem.* 305 (2009) 40–46. DOI: [10.1016/j.molcata.2008.10.047](https://doi.org/10.1016/j.molcata.2008.10.047)
- [97]. A.K. Aboul-Gheit, A.E. Awadallah, S.M. El-Kossy, A.-L.H. Mahmoud, *J. Nat. Gas Chem.* 17 (2008) 337–343. DOI: [10.1016/S1003-9953\(09\)60005-0](https://doi.org/10.1016/S1003-9953(09)60005-0)
- [98]. L. Wang, Y. Xu, S.-T. Wong, W. Cui, X. Guo, *Appl. Catal. A Gen.* 152 (1997) 173–182. DOI: [10.1016/S0926-860X\(96\)00366-3](https://doi.org/10.1016/S0926-860X(96)00366-3)
- [99]. R. Kojima, S. Kikuchi, H. Ma, J. Bai, M. Ichikawa, *Catal. Lett.* 110 (2006) 15–21. DOI: [10.1007/s10562-006-0087-x](https://doi.org/10.1007/s10562-006-0087-x)
- [100]. Y. Shu, Y. Xu, S.-T. Wong, L. Wang, X. Guo, *J. Catal.* 170 (1997) 11–19. DOI: [10.1006/jcat.1997.1726](https://doi.org/10.1006/jcat.1997.1726)
- [101]. A. Szöke, F. Solymosi, *Appl. Catal. A Gen.* 142 (1996) 361–374. DOI: [10.1016/0926-860X\(96\)00085-3](https://doi.org/10.1016/0926-860X(96)00085-3)
- [102]. H. Wang, Z. Liu, J. Schen, H. Liu, J. Zhang, *Catal. Commun.* 6 (2005) 343–346. DOI: [10.1016/j.catcom.2005.02.008](https://doi.org/10.1016/j.catcom.2005.02.008)
- [103]. L. Chen, L. Lin, Z. Xu, T. Zhang, X. Li, *Catal. Lett.* 39 (1996) 169–172. DOI: [10.1007/BF00805578](https://doi.org/10.1007/BF00805578)
- [104]. P.D. Sily, F.B. Noronha, F.B. Passos, *J. Nat. Gas Chem.* 15 (2006) 82–86. DOI: [10.1016/S1003-9953\(06\)60012-1](https://doi.org/10.1016/S1003-9953(06)60012-1)
- [105]. S. Majhi, P. Mohanty, H. Wang, K.K. Pant, *J. Energy Chem.* 22 (2013) 543–554. DOI: [10.1016/S2095-4956\(13\)60071-6](https://doi.org/10.1016/S2095-4956(13)60071-6)
- [106]. S. Li, C. Zhang, Q. Kan, D. Wang, T. Wu, L. Lin, *Appl. Catal. A Gen.* 187 (1999) 199–206. DOI: [10.1016/S0926-860X\(99\)00231-8](https://doi.org/10.1016/S0926-860X(99)00231-8)
- [107]. R. Baker, *J. Catal.* 26 (1972) 51–62. DOI: [10.1016/0021-9517\(72\)90032-2](https://doi.org/10.1016/0021-9517(72)90032-2)
- [108]. V.I. Zaikovskii, V.V. Chesnokov, R.A. Buyanov, L.M. Plyasova, *Kinet. Catal.* 41 (2000) 538–545. DOI: [10.1007/BF02756072](https://doi.org/10.1007/BF02756072)
- [109]. V.I. Zaikovskii, A.V. Vosmerikov, V.F. Anufrienko, L.L. Korobitsyna, E.G. Kodenev, G. V. Echevskii, N.T. Vasenin, S.P. Zhuravkov, Z.R. Ismagilov, V.N. Parmon, *Dokl. Phys. Chem.* 404 (2005) 201–204. DOI: [10.1007/s10634-005-0060-1](https://doi.org/10.1007/s10634-005-0060-1)
- [110]. V.I. Zaikovskii, A.V. Vosmerikov, V.F. Anufrienko, L.L. Korobitsyna, E.G. Kodenev, G.V. Echevskii, N.T. Vasenin, S.P. Zhuravkov, E.V. Matus, Z.R. Ismagilov, V.N. Parmon, *Kinet. Catal.* 47 (2006) 389–394. DOI: [10.1134/S0023158406030104](https://doi.org/10.1134/S0023158406030104)
- [111]. B. Li, S. Li, N. Li, H. Chen, W. Zhang, X. Bao, B. Lin, *Microp. Mesopor. Mat.* 88 (2006) 244–253. DOI: [10.1016/j.micromeso.2005.09.016](https://doi.org/10.1016/j.micromeso.2005.09.016)
- [112]. S. Li, D. Ma, Q. Kan, P. Wu, Y. Peng, C. Zhang, M. Li, Y. Fu, J. Shen, T. Wu, X. Bao, *React. Kinet. Catal. Lett.* 70 (2000) 349–356. DOI: [10.1023/A:1010309521261](https://doi.org/10.1023/A:1010309521261)
- [113]. Y. Xu, W. Liu, S.-T. Wong, L. Wang, X. Guo, *Catal. Lett.* 40 (1996) 207–214. DOI: [10.1007/BF00815284](https://doi.org/10.1007/BF00815284)
- [114]. S. De, J. Zhang, R. Luque, N. Yan, *Energy Environ. Sci.* 9 (2016) 3314–3347. DOI: [10.1039/C6EE02002J](https://doi.org/10.1039/C6EE02002J)
- [115]. V. Dal Santo, A. Gallo, A. Naldoni, M. Guidotti, R. Psaro, *Catal. Today* 197 (2012) 190–205. DOI: [10.1016/j.cattod.2012.07.037](https://doi.org/10.1016/j.cattod.2012.07.037)
- [116]. Y.H. (Cathy) Chin, D.L. King, H.S. Roh, Y. Wang, S.M. Heald, *J. Catal.* 244 (2006) 153–162. DOI: [10.1016/j.jcat.2006.08.016](https://doi.org/10.1016/j.jcat.2006.08.016)
- [117]. C. Xie, Y. Chen, Y. Li, X. Wang, C. Song, *Appl. Catal. A Gen.* 390 (2010) 210–218. DOI: [10.1016/j.apcata.2010.10.012](https://doi.org/10.1016/j.apcata.2010.10.012)
- [118]. E.C. Luna, A.M. Becerra, M.I. Dimitrijewits, *React. Kinet. Catal. Lett.* 67 (1999) 247–252. DOI: [10.1007/BF02475767](https://doi.org/10.1007/BF02475767)
- [119]. K. Yoshida, N. Begum, S. Ito, K. Tomishige, *Appl. Catal. A Gen.* 358 (2009) 186–192. DOI: [10.1016/j.apcata.2009.02.025](https://doi.org/10.1016/j.apcata.2009.02.025)
- [120]. J.S. Lisboa, L.E. Terra, P.R.J. Silva, H. Saitovitch, F.B. Passos, *Fuel Process. Technol.* 92 (2011) 2075–2082. DOI: [10.1016/j.fuproc.2011.06.011](https://doi.org/10.1016/j.fuproc.2011.06.011)
- [121]. I.Z. Ismagilov, E. V. Matus, V.V. Kuznetsov, N. Mota, R.M. Navarro, S.A. Yashnik, I.P. Prosvirin, M.A. Kerzhentsev, Z.R. Ismagilov, J.L.G. Fierro, *Appl. Catal. A Gen.* 481 (2014) 104–115. DOI: [10.1016/j.apcata.2014.04.042](https://doi.org/10.1016/j.apcata.2014.04.042)
- [122]. M.A. Mashkovtsev, A.K. Khudorozhkov, I.E. Beck, A.V. Porsin, I.P. Prosvirin, V.N. Rychkov, V.I. Bukhtiyarov, *Catal. Ind.* 3 (2011) 350–357. DOI: [10.1134/S2070050411040052](https://doi.org/10.1134/S2070050411040052)
- [123]. L. Ma, L. Yan, A.-H. Lu, Y. Ding, *RSC Adv.* 8 (2018) 8152–8163. DOI: [10.1039/C7RA12891F](https://doi.org/10.1039/C7RA12891F)
- [124]. X. Yu, F. Zhang, W. Chu, *RSC Adv.* 6 (2016) 70537–70546. DOI: [10.1039/C6RA12335J](https://doi.org/10.1039/C6RA12335J)
- [125]. J. Xu, W. Zhou, Z. Li, J. Wang, J. Ma, *Int. J. Hydrogen Energ.* 34 (2009) 6646–6654. DOI: [10.1016/j.ijhydene.2009.06.038](https://doi.org/10.1016/j.ijhydene.2009.06.038)
- [126]. S.C. Dantas, J.C. Escritori, R.R. Soares, C.E. Hori, *Chem. Eng. J.* 156 (2010) 380–387. DOI: [10.1016/j.cej.2009.10.047](https://doi.org/10.1016/j.cej.2009.10.047)

- [127]. N.N. Nichio, M.L. Casella, G.F. Santori, E.N. Ponzi, O.A. Ferretti, *Catal. Today* 62 (2000) 231–240. DOI: [10.1016/S0920-5861\(00\)00424-7](https://doi.org/10.1016/S0920-5861(00)00424-7)
- [128]. Z. Hou, O. Yokota, T. Tanaka, T. Yashima, *Appl. Surf. Sci.* 233 (2004) 58–68. DOI: [10.1016/j.apsusc.2004.03.223](https://doi.org/10.1016/j.apsusc.2004.03.223)
- [129]. E. Nikolla, J. Schwank, S. Linic, *J. Catal.* 250 (2007) 85–93. DOI: [10.1016/j.jcat.2007.04.020](https://doi.org/10.1016/j.jcat.2007.04.020)
- [130]. S. Saadi, B. Hinnemann, S. Helveg, C.C. Appel, F. Abild-Pedersen, J.K. Nørskov, *Surf. Sci.* 603 (2009) 762–770. DOI: [10.1016/j.susc.2009.01.018](https://doi.org/10.1016/j.susc.2009.01.018)
- [131]. F. Yang, D. Liu, H. Wang, X. Liu, J. Han, Q. Ge, X. Zhu, *J. Catal.* 349 (2017) 84–97. DOI: [10.1016/j.jcat.2017.01.001](https://doi.org/10.1016/j.jcat.2017.01.001)
- [132]. Z.O. Malaibari, A. Amin, E. Croiset, W. Epling, *Int. J. Hydrogen Energ.* 39 (2014) 10061–10073. DOI: [10.1016/j.ijhydene.2014.03.169](https://doi.org/10.1016/j.ijhydene.2014.03.169)
- [133]. A. Erhan Aksoylu, Z.I. Önsan, *Appl. Catal. A Gen.* 168 (1998) 399–407. DOI: [10.1016/S0926-860X\(97\)00370-0](https://doi.org/10.1016/S0926-860X(97)00370-0)
- [134]. B.S. Çağlayan, Z.I. Önsan, A.E. Aksoylu, *Catal. Lett.* 102 (2005) 63–67. DOI: [10.1007/s10562-005-5204-8](https://doi.org/10.1007/s10562-005-5204-8)
- [135]. M. Sharifi, M. Haghghi, F. Rahmani, S. Karimipour, *J. Nat. Gas Sci. Eng.* 21 (2014) 993–1004. DOI: [10.1016/j.jngse.2014.10.030](https://doi.org/10.1016/j.jngse.2014.10.030)
- [136]. J.A.C. Dias, J.M. Assaf, *Appl. Catal. A Gen.* 334 (2008) 243–250. DOI: [10.1016/j.apcata.2007.10.012](https://doi.org/10.1016/j.apcata.2007.10.012)
- [137]. M. Sankar, N. Dimitratos, P.J. Miedziak, P.P. Wells, C.J. Kiely, G.J. Hutchings, *Chem. Soc. Rev.* 41 (2012) 8099–8139. DOI: [10.1039/C2CS35296F](https://doi.org/10.1039/C2CS35296F)
- [138]. D. Li, T. Shishido, Y. Oumi, T. Sano, K. Takehira, *Appl. Catal. A Gen.* 332 (2007) 98–109. DOI: [10.1016/j.apcata.2007.08.008](https://doi.org/10.1016/j.apcata.2007.08.008)
- [139]. T. Miyata, D. Li, M. Shiraga, T. Shishido, Y. Oumi, T. Sano, K. Takehira, *Appl. Catal. A Gen.* 310 (2006) 97–104. DOI: [10.1016/j.apcata.2006.05.022](https://doi.org/10.1016/j.apcata.2006.05.022)
- [140]. L.P.R. Profeti, E.A. Ticianelli, E.M. Assaf, I. De Qui, C. Sp, *Int. J. Hydrogen Energ.* 34 (2009) 5049–5060. DOI: [10.1016/j.ijhydene.2009.03.050](https://doi.org/10.1016/j.ijhydene.2009.03.050)
- [141]. D. Li, Y. Nakagawa, K. Tomishige, *Chinese J. Catal.* 33 (2012) 583–594. DOI: [10.1016/S1872-2067\(11\)60359-8](https://doi.org/10.1016/S1872-2067(11)60359-8)
- [142]. Y. Mukainakano, K. Yoshida, K. Okumura, K. Kunimori, K. Tomishige, *Catal. Today* 132 (2008) 101–108. DOI: [10.1016/j.cattod.2007.12.031](https://doi.org/10.1016/j.cattod.2007.12.031)
- [143]. Y. Mukainakano, K. Yoshida, S. Kado, K. Okumura, K. Kunimori, K. Tomishige, *Chem. Eng. Sci.* 63 (2008) 4891–4901. DOI: [10.1016/j.ces.2007.06.003](https://doi.org/10.1016/j.ces.2007.06.003)
- [144]. K. Yoshida, K. Okumura, T. Miyao, S. Naito, S. Ito, K. Kunimori, K. Tomishige, *Appl. Catal. A Gen.* 351 (2008) 217–225. DOI: [10.1016/j.apcata.2008.09.014](https://doi.org/10.1016/j.apcata.2008.09.014)
- [145]. J.A. Montoya, E. Romero-Pascual, C. Gimon, P. Del Angel, A. Monzon, *Catal. Today* 63 (2000) 71–85. DOI: [10.1016/S0920-5861\(00\)00447-8](https://doi.org/10.1016/S0920-5861(00)00447-8)
- [146]. B. Li, R. Watanabe, K. Maruyama, K. Kunimori, K. Tomishige, *Catal. Today* 104 (2005) 7–17. DOI: [10.1016/j.cattod.2005.03.037](https://doi.org/10.1016/j.cattod.2005.03.037)
- [147]. M.A. Kerzhentsev, E.V. Matus, I.A. Rundau, V.V. Kuznetsov, I.Z. Ismagilov, V.A. Ushakov, S.A. Yashnik, Z.R. Ismagilov, *Kinet. Catal.* 58 (2017) 601–609. DOI: [10.1134/S002315841705010X](https://doi.org/10.1134/S002315841705010X)
- [148]. J. Requies, M.A. Cabrero, V.L. Barrio, M.B. Güemez, J.F. Cambra, P.L. Arias, F.J. Pérez-Alonso, M. Ojeda, M.A. Peña, J.L.G. Fierro, *Appl. Catal. A Gen.* 289 (2005) 214–223. DOI: [10.1016/j.apcata.2005.05.002](https://doi.org/10.1016/j.apcata.2005.05.002)
- [149]. K. Rida, M.A. Peña, E. Sastre, A. Martínez-Arias, *J. Rare Earth.* 30 (2012) 210–216. DOI: [10.1016/S1002-0721\(12\)60025-8](https://doi.org/10.1016/S1002-0721(12)60025-8)
- [150]. Y. Wang, J. Zhu, X. Yang, L. Lu, X. Wang, *Material. Research Bull.* 41 (2006) 1565–1570. DOI: [10.1016/j.materresbull.2005.11.017](https://doi.org/10.1016/j.materresbull.2005.11.017)
- [151]. C.R.B. Silva, L. Da Conceição, N.F.P. Ribeiro, M.M.V.M. Souza, *Catal. Commun.* 12 (2011) 665–668. DOI: [10.1016/j.catcom.2010.12.025](https://doi.org/10.1016/j.catcom.2010.12.025)
- [152]. R.D. Shannon, *Acta Cryst.* 32 (1976) 751–767. DOI: [10.1107/S0567739476001551](https://doi.org/10.1107/S0567739476001551)
- [153]. A. Vamvakarios, S.D.M. Jacques, M. Di Michiel, D. Matras, V. Middelkoop, I.Z. Ismagilov, E.V. Matus, V.V. Kuznetsov, J. Drnec, P. Senecal, A.M. Beale, *Nat. Commun.* 9 (2018) 4751. DOI: [10.1038/s41467-018-07046-8](https://doi.org/10.1038/s41467-018-07046-8)
- [154]. X. Liu, B. Cheng, J. Hu, H. Qin, M. Jiang, *Sensor. Actuat. B Chem.* 129 (2008) 53–58. DOI: [10.1016/j.snb.2007.07.102](https://doi.org/10.1016/j.snb.2007.07.102)
- [155]. H. Provendier, C. Petit, C. Estournès, S. Libs, A. Kiennemann, *Appl. Catal. A Gen.* 180 (1999) 163–173. DOI: [10.1016/S0926-860X\(98\)00343-3](https://doi.org/10.1016/S0926-860X(98)00343-3)
- [156]. I.Z. Ismagilov, E.V. Matus, V.V. Kuznetsov, N. Mota, R.M. Navarro, M.A. Kerzhentsev, Z.R. Ismagilov, J.L.G. Fierro, *Catal. Today* 210 (2013) 10–18. DOI: [10.1016/j.cattod.2012.12.007](https://doi.org/10.1016/j.cattod.2012.12.007)
- [157]. D. Hufschmidt, L.F. Bobadilla, F. Romero-Sarria, M.A. Centeno, J.A. Odriozola, M. Montes, E. Falabella, *Catal. Today* 149 (2010) 394–400. DOI: [10.1016/j.cattod.2009.06.002](https://doi.org/10.1016/j.cattod.2009.06.002)